

Deglacial and postglacial evolution of the Pingualuit Crater Lake basin, northern Québec (Canada)



Pierre-Arnaud Desiège^{a,b,*}, Patrick Lajeunesse^{b,c}, Guillaume St-Onge^{a,b}, Alexandre Normandeau^b, Grégoire Ledoux^c, Hervé Guyard^{a,b,d}, Reinhard Pienitz^c

^a Institut des sciences de la mer de Rimouski (ISMER), Canada Research Chair in Marine Geology, Université du Québec à Rimouski, Rimouski, Canada

^b GEOTOP Research Center, Canada

^c Centre d'études Nordiques (CEN) & Département de Géographie, Université Laval, Québec, Canada

^d Institut de Physique du Globe de Paris, Sorbonne Paris Cité, Université Paris Diderot, UMR CNRS 7154, Paris, France

ARTICLE INFO

Article history:

Received 15 January 2015

Received in revised form 9 July 2015

Accepted 10 July 2015

Available online 29 July 2015

Keywords:

lake levels

Mass movements

Laurentide Ice Sheet

Sedimentological processes

LiDAR

Arctic

ABSTRACT

The Pingualuit Crater, located in the Ungava Peninsula (northern Québec, Canada) is a 1.4-Ma-old impact crater hosting a ~245-m-deep lake. The lake has a great potential to preserve unique paleoclimatic and paleoecological sedimentary records of the last glacial/interglacial cycles in the terrestrial Canadian Arctic. In order to investigate the stratigraphy in the lake and the late Quaternary glacial history of the Pingualuit Crater, this study compiles data from three expeditions carried out in May 2007 (~9-m-long sediment core), in August 2010 (~50 km of seismic lines), and in September 2012 (high-resolution terrestrial LiDAR topography of the inner slopes). Despite the weak penetration (~10 m) of the 3.5-kHz subbottom profiling caused by the presence of boulders in the sedimentary column, seismic data coupled with the stratigraphy established from the sediment core enabled the identification of two glaciolacustrine units deposited during the final stages of the Laurentide Ice Sheet (LIS) retreat in the crater. Two episodes of postglacial mass wasting events were also identified on the slopes and in the deep basin of the crater. The high-resolution topography of the internal slopes of the crater generated from the LiDAR data permitted the confirmation of a paleolake level at 545 m and determination of the elevation of drainage outlets. Together with the mapping of glacial and deglacial landforms from air photographs, the LiDAR data allowed the development of a new deglaciation and drainage scenario for the Pingualuit Crater Lake and surrounding area. The model proposes three main phases of lake drainage, based on the activation of seven outlets following the retreat of the LIS front toward the southwest. Finally, as opposed to other high-latitude crater lake basins such as Lake El'gygytyn or Laguna Potrok Aike where high-resolution paleoclimatic records were obtained owing to high sediment accumulation rates, the seismic data from the Pingualuit Crater Lake suggest extremely low sedimentation rates after the retreat of the LIS owing to the absence of tributaries.

© 2015 Elsevier B.V. All rights reserved.

1. Introduction

High-latitude lakes contain excellent archives of past climatic and environmental variations owing to the sediments they can preserve (Pienitz et al., 2004, 2008). In recent years, the Pingualuit Crater Lake (Nunavik; Fig. 1) has sparked a renewed interest in paleoclimatology research in the Ungava Peninsula (Black et al., 2010, 2012; Girard-Cloutier, 2011; Guyard et al., 2011, 2014; Luoto et al., 2013). Despite the presence of the Laurentide Ice Sheet during the Last Glacial Maximum (~21,000 years ago; Clark et al., 2009), the morphology of the crater likely favored the existence of a subglacial lake in the Pingualuit

Crater, precluding glacial erosion of the bottom sediments (Bouchard, 1989b; Guyard et al., 2011). These characteristics give the Pingualuit Crater Lake sediments the potential to record successions of glacial/interglacial periods in the Ungava Peninsula since its formation 1.4 Ma ago (Bouchard, 1989b). Furthermore, the Pingualuit Crater Lake has similar characteristics to lakes recently studied in the context of International Continental scientific Drilling Program (ICDP) projects for their potential in paleoclimatic research, such as the El'gygytyn Crater Lake in 2008/09 (e.g., Melles et al., 2012) and Laguna Potrok Aike in 2008 (e.g., Zolitschka et al., 2013, and papers in the special issue). El'gygytyn Crater Lake, also a meteoritic impact basin located in the Arctic (67.5°N., 172°E.), escaped Northern Hemisphere glaciation because of its location in the center of Beringia (Brigham-Grette et al., 2007). Laguna Potrok Aike, located in southeastern Patagonia (Argentina), and the Pingualuit Crater Lake share a similar morphology with a high depth-to-area ratio, allowing the potential accumulation of a long sedimentary record

* Corresponding author at: Institut des Sciences de la mer de Rimouski, Université du Québec à Rimouski, 310 allée des Ursulines, Rimouski, Québec G5L 3A1, Canada.

E-mail address: Pierre-Arnaud.Desiège@uqar.ca (P.-A. Desiège).

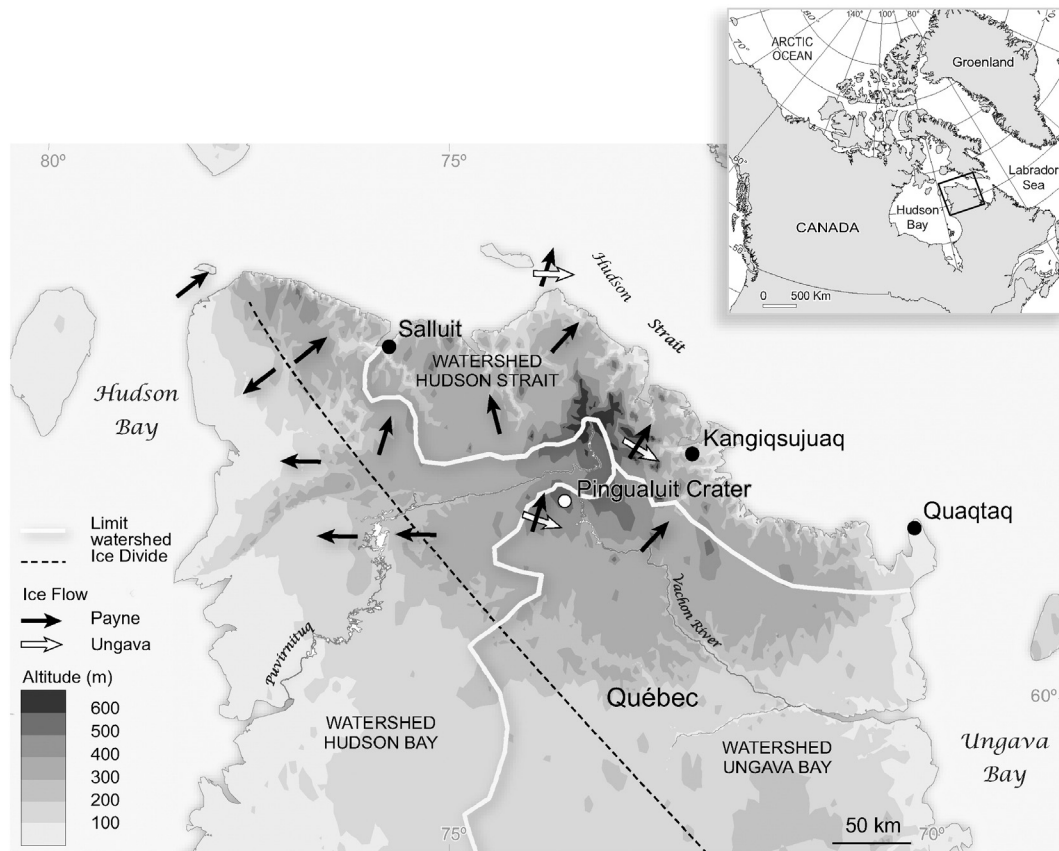


Fig. 1. Location of the Pingualuit Crater Lake in the Ungava Peninsula. Black and white arrows show the main ice flow directions (Payne and Ungava) based on depositional and erosional landforms (Bouchard and Marcotte, 1986; Daigneault and Bouchard, 2004). The dashed line illustrates the ice divide (Daigneault and Bouchard, 2004), and the white line marks the limit between the Ungava Bay, and Hudson Bay watersheds. Realization: Département de Géographie, Université Laval, 2013.

(Bouchard, 1989a; Anselmetti et al., 2009). The long sediment records obtained from such deep and old crater lake systems yield invaluable insights into the linkages between climate forcing mechanisms and global paleoenvironmental changes, thereby improving the output of regional and global climate models and contributing to a better understanding of past, present, and future climate change (Pienitz et al., 2008).

This study aims to investigate the late Quaternary glacial and deglacial history of the Pingualuit Crater Lake basin and to better understand the sedimentary infill of the lake based on recently acquired seismic and LiDAR data. These new and high resolution data sets, together with regional mapping of glacial and deglacial landforms based on aerial photographs, will contextualize and update the paleoclimatic archives recovered in the lake (Guyard et al., 2011, 2014; Black et al., 2012; Luoto et al., 2013), and allow reconstructing precisely the successive stages of crater deglaciation and the resulting rapid drainage events of the lake, first suggested by Bouchard and Saarnisto (1989). Indeed, the high-resolution topography of the inner crater, generated with the LiDAR data, confirms the presence of paleoshorelines visually tracked by Bouchard and Saarnisto (1989) and improves the resolution of elevation measurements from ± 5 to 1 m.

2. Study area

The Pingualuit Crater, located in the Ungava Peninsula (Nunavik, Canada; Fig. 1) is a simple crater created by a meteoritic impact ~1.4 million years ago (Grieve et al., 1991). The crater is a ~410-m-deep (rim-to-basin) and 3.4-km-wide (rim-to-rim) near circular depression whose rim reaches a maximum elevation of 657 m above sea level (asl), making it one of the highest peaks in Ungava. This summit rises

to 163 m above the surface (494 m asl) of an ultraoligotrophic ~245-m-deep and 2.8-km-wide lake surrounded by the crater. Since the last deglaciation the lake has been a closed sedimentary basin with no tributaries as the lake is only fed by atmospheric precipitation (Guyard et al., 2011). However, $\delta^{18}\text{O}$ measurements made by Ouellet et al. (1989) in the Pingualuit Crater Lake and adjacent Lake Laflamme suggest a potential underground (cryptorheic) drainage system across a fault plane linking both lakes and allowing flows from the crater lake to Lake Laflamme (Currie, 1965). The water flows of the Pingualuit Crater area are drained by the Vachon River across the Ungava Bay catchment basin. The northernmost part of this area is adjacent to the Puvirnituk River, one of the main rivers of the Hudson Bay catchment basin (Fig. 1; Daigneault, 2008).

The crater is located in the Archean-age Superior Province of the Canadian Shield. The lithology in the area south of the Cape-Smith Belt, where the crater is situated, is dominated by tonalitic and granitic gneiss (St-Onge and Lucas, 1990; Daigneault, 2008). Around the crater, the bedrock geology also includes plutonic rocks, mostly granitoids, crosscut by mafic dykes (Currie, 1965; Bouchard and Marsan, 1989). The ground surface consists of blocks, gravels, and a 0–2 m-thick discontinuous till. Furthermore, dozens of erratic boulders of dolostone from the Proterozoic Cape-Smith Belt, located ~40 km north, have been counted in the crater area (Bouchard et al., 1989). The rim and steep inner slopes (26–35°) are also strewn with boulders and rocks mineralized with epidote, hematite, and sericite, probably produced by alteration (Currie, 1965). These slopes terminate on an asymmetric basin consisting of a plateau in the southwest part of the lake and a deep basin in the northeast part of the lake (Bouchard and Marsan, 1989). Bouchard (1989a) explains this morphology by high sediment input

from the southwest during the last deglaciation. Interpretation of seismic data acquired during a survey in 1988 by [Moussawi and Tessier \(1989\)](#) suggests thick deposits of till and/or gravels intersected by fine clay layers (thickness between 1 and 2 m). The chaotic seismic signal furthermore reveals the presence of blocks throughout the sediments with the exception of the upper 25 m of the deep basin, where sediments are finer. Reflectors indicate a potential accumulation of at least 73 m of sediments on the plateau and 93 m in the deep basin ([Bouchard, 1989a; Moussawi and Tessier, 1989](#)). [Bouchard \(1989a\)](#) explained the presence of thick and coarse till deposits in the crater by a rain-out and reworking of sediments from melting ice and/or by dense flows originating from glacial retreat. The stratigraphy of a ~9-m-long core retrieved in 2007 from the deep basin reveals subglacial and proglacial lacustrine depositional conditions during the last deglaciation and organic-rich intervals corresponding to ice-free conditions during postglacial times ([Guyard et al., 2011, 2014; Luoto et al., 2013](#)). This stratigraphy will be integrated with the discussion of seismic surveys hereinafter.

2.1. Regional glacial/deglacial history

During the last glaciation, northern Ungava remained glaciated from the end of the Sangamonian (marine isotopic substage 5e; ~123,000 yr; [Lisiecki and Raymo, 2005](#)) to the Holocene deglaciation ([Daigneault, 2008](#)). In the Pingualuit Crater Lake basin, two distinct glacial movements have characterized the last glaciation: an older *Ungava* ice flow phase and a younger *Payne* phase ([Gray and Lauriol, 1985; Bouchard and Marcotte, 1986](#)). The older of the two originated from the Ungava center in the central part of the Ungava Peninsula and was oriented southeast (azimuth 110°) in the study area, whereas the younger originating from the Payne center was oriented northeast (azimuth 45°) ([Fig. 1; Currie, 1965; Bouchard et al., 1989; Daigneault and Bouchard, 2004](#)). During this second glacial movement, the Payne flow covered the main part of the Ungava Peninsula. This relative chronology is supported in the crater area by the greatest abundance of glacial landforms being associated with younger Payne flow ([Bouchard et al., 1989; Daigneault and Bouchard, 2004](#)).

Deglaciation of the Ungava Peninsula began on the southern coast of the Hudson Strait in the northwestern and northern extremities of the peninsula between 10.5 and 7 ky BP, and progressed toward the Ungava plateau ([Gray and Lauriol, 1985; Dyke and Prest, 1987; Lauriol and Gray, 1987; Bruneau and Gray, 1997; Gray, 2001; Daigneault and Bouchard, 2004; Saulnier-Talbot and Pienitz, 2010; Occhietti et al., 2011](#)). The orientation of glacial retreat was directed along a NW–SE axis located west of the ice divide ([Fig. 1; Prest, 1969; Daigneault, 2008](#)). Furthermore, [Clark et al. \(2000\)](#) suggested for the entire Québec-Labrador Sector of the Laurentide Ice Sheet (LIS), including the Ungava Peninsula, a progressive fragmentation of the ice sheet into separate local ice masses during its retreat inland. In the Pingualuit Crater, AMS ¹⁴C dating and the multiproxy paleoenvironmental reconstruction performed by [Guyard et al. \(2011\)](#) on the ~9-m sediment core collected in the deep basin in 2007 suggest that the LIS retreated from the crater area around 6840 ± 100 cal y BP (6000 ± 40 ¹⁴C y BP).

The Pingualuit Crater Lake has sustained several rapid drainage events during deglaciation as revealed by the three paleoshorelines (574, 544, and 514 m) on the internal slopes of the crater and the outwash channels on the external slopes and grounds surrounding the crater ([Bouchard and Saarnisto, 1989](#)). According to these authors, the drainages have occurred through several of the 10 channels in the crater rim (i.e., outlets) during four main phases of glacial retreat in the area ([Fig. 2](#)). During the first phase, the U-shaped and highest channels 6 and 7 (respectively about 608 and 596 m) were cleared of ice and drained small volumes of the lake waters. As the glacial retreat progressed to phase 2, the opening of outlets 5 and 8 reduced the lake level by about 20 m ([Fig. 2](#)). Outflows through channels 5 and 8 were torrential, with a strong erosive power causing the development of

outflow systems at the base of the crater. The highest paleoshoreline (574 ± 5 m asl) observed by [Bouchard and Saarnisto \(1989\)](#) on the northern half of the crater was formed during this second phase. The paleoshorelines constitute discontinued lines formed by benches sometimes associated with gravel veneers ([Bouchard and Saarnisto, 1989](#)). The glacial retreat to phase 3 caused the draining of outlets 5 and 8 and the freeing of western channels 4 and 3 and eastern channels 9 and 10 ([Fig. 2](#)). However, channels 9 and 10 do not appear to have been affected by drainage events owing to their high elevation (601 m) precluding contact with lake waters (between 574 and 544 ± 5 m during phase 3). [Bouchard and Saarnisto \(1989\)](#) have explained the existence of an outflow system at the base of the crater near channel 10 by a sub- and proglacial drainage system independent of the crater lake during glacial retreat. During phase 4, the lake was totally ice free but southern channels 2 and 1 were not affected by drainage, their elevation being higher than that of channel 3 ([Fig. 2](#)). Torrential outflows through channel 3 persisted during and after phase 4, allowing a connection with Lake Laflamme. Finally, the link was interrupted when the lake level dropped beneath that of the second paleoshoreline (544 ± 5 m asl), abandoning the lowermost outlet (channel 3 at 553 m). This paleoshoreline is the most pronounced with a level of washed boulders tied to the cover lichen that differs from the adjacent block, visible all around the crater. A ledge about 5 m wide also characterizes this paleolake level in the eastern part of the crater. The third paleoshoreline (around 509–514 m asl) is poorly developed and barely observable in some parts of the internal slopes ([Bouchard and Saarnisto, 1989](#)).

During deglaciation, part of the territory around the crater was covered by proglacial lakes adjoining the ice margin ([Daigneault, 2008](#)). These lakes were located especially upstream of the Vachon and Puvirnituk Rivers ([Prest, 1975; Daigneault, 1993, 2008](#)). Nevertheless, none of these lakes appear to have reached a sufficient elevation to allow an overflow into the Pingualuit Crater Lake. Indeed, the maximal levels of proglacial lakes Saint-Germain and Laflamme (respectively 520 and 515 m) ([Fig. 2](#)) bordering the crater were not high enough to inundate the minimum elevation of the rim (channel 3 at 553 ± 5 m) ([Bouchard and Saarnisto, 1989; Daigneault, 2008](#)).

3. Methodology

3.1. Aerial photo and satellite imagery mapping of landforms

In order to identify glacial and deglacial landforms, three series of medium scale aerial photographs (1:20,000 and 1:30,000) from the *GéoStat* Center (U. Laval) and *Géomathèque*® were selected and digitized with a 350 dpi resolution. The 26 air photos used cover an area of ~455 km², mainly in the north, east, and west parts of the crater area. Analysis of Landsat 7 satellite images and 2012 fieldwork observations (see below) were used to complete the aerial photography interpretation. Landsat images (spectral band 1 and composite 7-4-3) from the *GeoBase* database (<http://www.geobase.ca>; Natural Resources Canada) round out the study of areas not covered by air photos but only allow the mapping of large-scale landforms ([Lajeunesse, 2008](#)). Furthermore, analysis and interpretation of landforms were based on previous documentation and a surficial geology map of the eastern part of the Ungava Peninsula ([Daigneault, 1997](#)). All landforms related to glacial and deglacial processes were identified on a map of a DEM of the Pingualuit crater area generated from elevation data of the *GeoBase* database.

3.2. Terrestrial LiDAR mapping

In September 2012, a survey was conducted to record the high-resolution topography of the internal slopes of the crater using a terrestrial LiDAR. A total of 35 surveys were completed with the *ILRIS-3D* laser scanning system from *Optech Inc.* These scans were recorded from 19

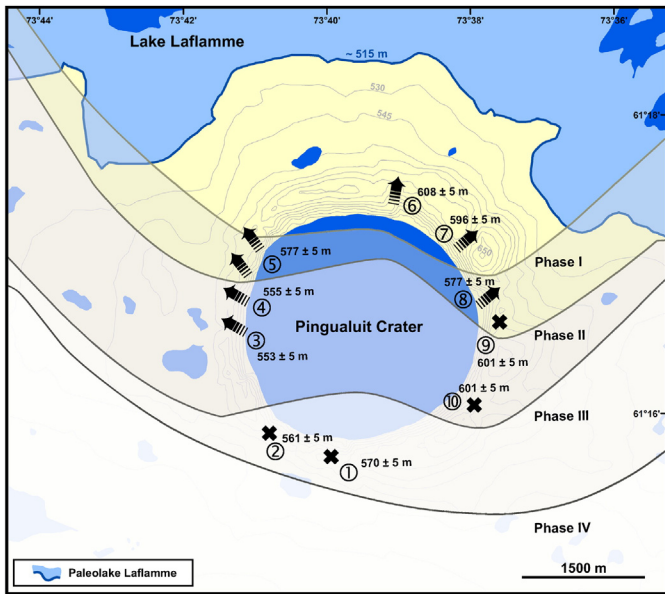


Fig. 2. Conceptual model for deglaciation of the Pingualuit Crater Lake suggested by Bouchard and Saarnisto (1989). Black arrows show the crater rim channels hosting outflows, whereas black crosses illustrate valleys not affected by drainage. The numbers indicate the 10 valleys in the crater rim and their elevations according to Bouchard and Saarnisto (1989). Also illustrated is the proglacial Lake Laflamme at its maximal level (~515 m) (Bouchard and Saarnisto, 1989). The four phases represent the main steps of glacial retreat and were associated with drainage events of the lake (see text for details).

different sites around the crater rim on the top of the internal slopes; the coordinates of each site were measured by GPS (Fig. 3). Spacing among sites is at most 600 m to maximize overlap between scans for the merge step. The scanning range of a survey covers up to 1500 m of the slope in the highest reflectivity conditions (Optech Inc, 2008). The three-dimensional point clouds acquired with the terrestrial LiDAR were imported and merged with Polyworks CAD (computer-aided design) software from Innovmetric Inc. To facilitate the merging process, a site was selected to generate an absolute coordinate (i.e., 0; 0; 0) and all other site coordinates were transformed accordingly. A scan recorded from this selected site was used as a base for merging the other scans. The point clouds were manually aligned and then merged using the Best-Fit function from the IMAAlign Polyworks software to achieve the highest convergence. The large ASCII file generated during this process was converted to LAS (LASer) file format to create a ground surface (DEM) of 0.5-m vertical and horizontal resolution using LP360 from the QCoherent software (Fig. 4). The resulting DEM was then exported into ArcGIS® software to analyze the internal slopes of the crater and to determine the elevation of various outlets.

3.3. Bathymetry and seismic acquisition-stratigraphy

About 50 km of subbottom profiles (Fig. 3) were collected in the Pingualuit Crater Lake in August 2010 using a Knudsen Chirp 3212 system with a frequency of 3.5 kHz (Ledoux et al., 2011). The subbottom profiler data were integrated and analyzed using The Kingdom Suite® software (IHS). Identified seismic horizons were exported into ArcGIS® to generate isopach maps for each unit. The acoustic travel times were converted into depth using p -wave velocities of $1420 \text{ m} \cdot \text{s}^{-1}$ for water depths and $1500 \text{ m} \cdot \text{s}^{-1}$ for the determination of sedimentary unit thickness, respectively (Moussawi and Tessier, 1989; Guyard et al., 2011). Interpretation of the observed units was completed using the correlation between seismic transects and stratigraphy of the ~9-m sediment core described by Guyard et al. (2011). The ~300-m meshing (Fig. 3) was used to produce a mid-resolution bathymetric map of the lake.

4. Results

4.1. Glacial geomorphology

4.1.1. Streamlined forms

Several streamlined forms compose the landscape in the Pingualuit Crater area. They are mainly gathered in the eastern sector of Lake St-Germain and Vachon River and to a lesser extent NE of Pingualuit Crater (Fig. 4). According to Daigneault (2008), the streamlined forms are principally drumlins and drumlinoids in the study area. Their size varies between 350 and 1000 m long and 100 and 400 m wide, with a maximum height of 10 m (Fig. 5B; Daigneault, 2008). The overall orientation of the streamlined forms matches with the main axis of the Payne ice flow, i.e., toward the NE (Fig. 1).

4.1.2. Hummocky moraines

Hummocky moraines are gathered in a sector located 1 km NE of the Pingualuit Crater (Fig. 5A). Hummocky moraines form irregular mounds or small ridges of till interrupted by depressions, which are occasionally occupied by ponds. The mounds never exceed 250 m in width and 5 m in height (Daigneault, 2008). This morphology extends over less than 25 km^2 with a maximum length of ~9 km and a maximum width of ~3 km (Fig. 4). In the central part of the hummocky moraines sector, the hummocks are poorly developed and less abundant, whereas in the eastern and western part of the area, the boundary between the moraine and the neighboring ground is clearly defined.

4.1.3. Esker

One short esker can be mapped about 3 km northeast of the crater (Fig. 5E). While esker segments of the eastern coast of Hudson Bay can reach lengths of 40 km (Lajeunesse, 2008), the segment observed in the area is <700-m-long. The esker appears to have a northeast direction, i.e., parallel to the direction of the Payne glaciation flow (Bouchard et al., 1989).

4.1.4. Proglacial lake paleoshorelines

Numerous paleoshorelines have been identified on the aerial photos in a small stretch located between the southern part of Lake St-Germain and the northernmost part of the Vachon River (Fig. 4). Paleoshorelines are also noticeable to a lesser extent at the foot and on the external slopes of the northern part of the Pingualuit Crater, near Lake Laflamme (Daigneault, 2008). Paleoshorelines appear as linear sections, parallel to contour lines, marking a break in slope (Fig. 5B). The linear section can occasionally be observed on aerial photos by change in tones caused by the scarp created by the erosive action of swash and/or seasonal ice on the shore. In the Lake St-Germain area, paleoshoreline elevation varies from 490 to 520 m. However, the characterization of the elevations of the paleoshorelines could be affected by glacioisostatic rebound following the deglaciation of the Ungava Peninsula (Matthews, 1967; Gray et al., 1993). The morphology of these paleolake levels consists of many gravelly beach deposits on both slopes of the southern part of Lake St-Germain (Daigneault, 2008). In the Lake Laflamme area, two major paleoshorelines are observed on aerial photos and measurements of the DEM. The first group of paleoshorelines, located in close proximity to the modern shores of Lake Laflamme, have an elevation of ~505 m. The second group, located on the external slopes of the Pingualuit Crater, have the highest paleoshorelines located at 545 m (Fig. 5C). These paleoshorelines are similar in configuration to those described above, with linear sections essentially perpendicular to the slope. They are characterized by a break in slope, appearing in the photos as darker colors because of the shade they cast. The depression produced by the break in slope can in some cases contain snow banks persisting late into the summer (Fig. 5C).

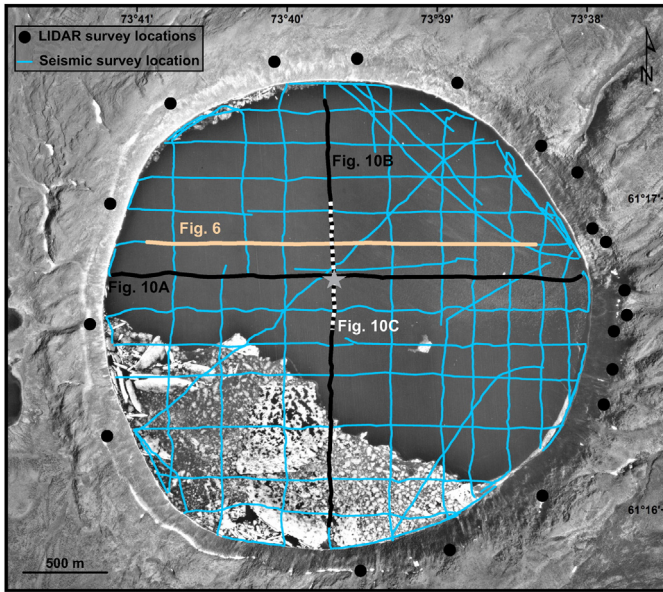


Fig. 3. Location on an aerial photograph (1:20,000; 13 August 1972) of seismic-reflection profiles collected in August 2010 (Ledoux et al., 2011), the sediment core collected in May 2007 (gray star), and LiDAR survey sites accomplished in September 2012.

4.2. Morphology and deglacial hydrology of Pingualuit Crater Lake

4.2.1. Topography–bathymetry model of the Pingualuit Crater

The entire inner part of the Pingualuit Crater was mapped for the first time using bathymetry coupled with the high-resolution topography of the internal slopes from LiDAR data (Fig. 6). The model confirmed the asymmetry of the crater with a shallower plateau in the south-southwestern part and a deeper basin in the northern part (Bouchard and Marsan, 1989). Furthermore, the morphology of the crater presents steep slopes flattened close to the floor and indicates no discrepancy between the emerged and the submerged slopes.

4.2.2. Pingualuit Crater Lake paleoshorelines

The paleoshorelines are ascertained from the LiDAR data based on three parameters: the identification of a break in slope or depressions, the continuity of a notch over several dozen meters, and the presence of equal elevation depressions at different sectors of the crater (preferentially opposite). The LiDAR data indicate several paleoshorelines along the internal slopes of the crater. Among the four paleoshoreline segments identified, three of them are located in the northeastern sector of the crater, while a fourth is located in the western sector (Fig. 7). The slope break and notches typical of paleoshorelines can be distinctly observed on the DEM processed from the LiDAR data (Fig. 8). The longest identifiable segment (Fig. 8B) measures ~150 m and the shortest is < 50 m. All four paleoshorelines have the same elevation of 545 m within a margin of error of 1 m (twice the DEM resolution). Existence of several paleoshorelines with the same elevation at different sites (northeast and west sectors) attests to a paleolake level at 545 m as suggested by Bouchard and Saarnisto (544 ± 5 m; 1989).

4.2.3. Characterization of the outlets

The outlets form U- or V-shaped channels cutting the rim of the crater. Ten outlets are recognizable around the rim (Fig. 2). Only seven are described in this study according to the criterion that they were potentially active during the last glacial retreat (Fig. 7). These outlets have the most pronounced channel profiles and are associated with traces of outflow on the external slopes of the crater (Fig. 5D). The channels located in the western sector of the crater are the lowest with values ranging from 546 to 575 m asl, whereas

elevation of the outlets in the eastern sector are the highest with values ranging from 575 to 599 m (Fig. 7). Owing to the very steep form of the lowest channel 3 (546 m asl) preventing an optimum coverage by the LiDAR, it is conceivable that the threshold of this channel is slightly underestimated by a few meters (Bouchard and Saarnisto (1989) mentioned the elevation of this channel at 553 m using geodetic surveys conducted in the early 1960s).

4.2.4. Pingualuit Crater Lake-deglaciation outflow marks

Three outflow systems formed by channels linked with outlets from the crater can be clearly observed on aerial photographs (Fig. 4). The first channel system, located in the western sector of the crater, connects western outlets with Lake Laflamme (Fig. 5D). Closer to the crater, the system is made up by two paleotributaries linked to outlets. The first is poorly demarcated and wide; it is linked with outlet 3 at 546 m asl and partially linked to outlet 4 at 556 m asl. Outlet 4 also flows into the second tributary with the western outlets 5 at 575 m asl. Indeed, in the downstream section of outlet 4, the outflow divides into two parts. The second tributary, more discernible, incises alongside the external slope of the crater and then diverges at the level of the southern outlet 5. The two paleotributaries merge to form a ~2-km-long narrow channel. At just <1 km from the present shoreline of Lake Laflamme, this channel disperses and divides into several small channels joining the lake. The surface affected by these outflow channels has a delta form with a low difference in elevation.

The second channel system, located in the northeastern sector of the crater area, connects eastern outlets at 597 and 575 m asl (respectively outlets 7 and 8) with the upstream part of the Vachon River (Fig. 4). An easily traced channel starts at each outlet. A few hundred meters from the external slopes, traces of outflow become more difficult to identify. The connection between outlet 8 and the channel is marked on the external slopes by a noticeable depression covered by washed boulders. Then the channel disperses and the flow paths appear to move northward to reach the second channel, connected to outlet 7, and the Vachon River.

The last channel is located in the southeastern sector of the crater at the mouth of outlet 10 at 599 m asl. At the end of the outlet, the outflows facing toward the northeast are characterized by a channel over 1 km long, segmented by several breaks in the slope, and covered by washed boulders (Fig. 9). The presence of washed boulders is quite recurrent at the end of outlets, in the channels on the external slopes, and at the base of the slopes. The *washed* appearance of boulders, likely created as a result of strong outflows, is amplified by the preservation of snow banks in the depressions, which probably precludes or modifies the development of lichen on the blocks (Bouchard and Saarnisto, 1989). At the base of the crater, this channel widens and divides into numerous distinct channels. The channel network enlarges with distance from the crater to reach a maximum width of ~700 m. Here the bedrock clearly appears as a white elongated and irregular grooves area on aerial photos. Flows have washed-out the till-covered bedrock and eroded it to form furrows on its surface. About 4 km east of the crater, traces made by flows converge over 2 km to reach the Vachon River with a width of ~200 m. In this area, the boundaries between the parts affected and unaffected by flows are clearly visible owing to extremely straight breaks in slope between them. In the downstream section of this channel system, the outflow marks are in contact with the esker (Fig. 5E). Indeed, the esker borders the northern limit of the channel system in this area and has a similar orientation (northeast direction) to these flow tracks. Furthermore, the irregular morphology of the short esker seems to coincide with winding marks of the channels.

5. Seismostratigraphy

Seismic reflection data allowed the identification of three seismic units and two types of mass movements (Fig. 10C). Nonetheless, the

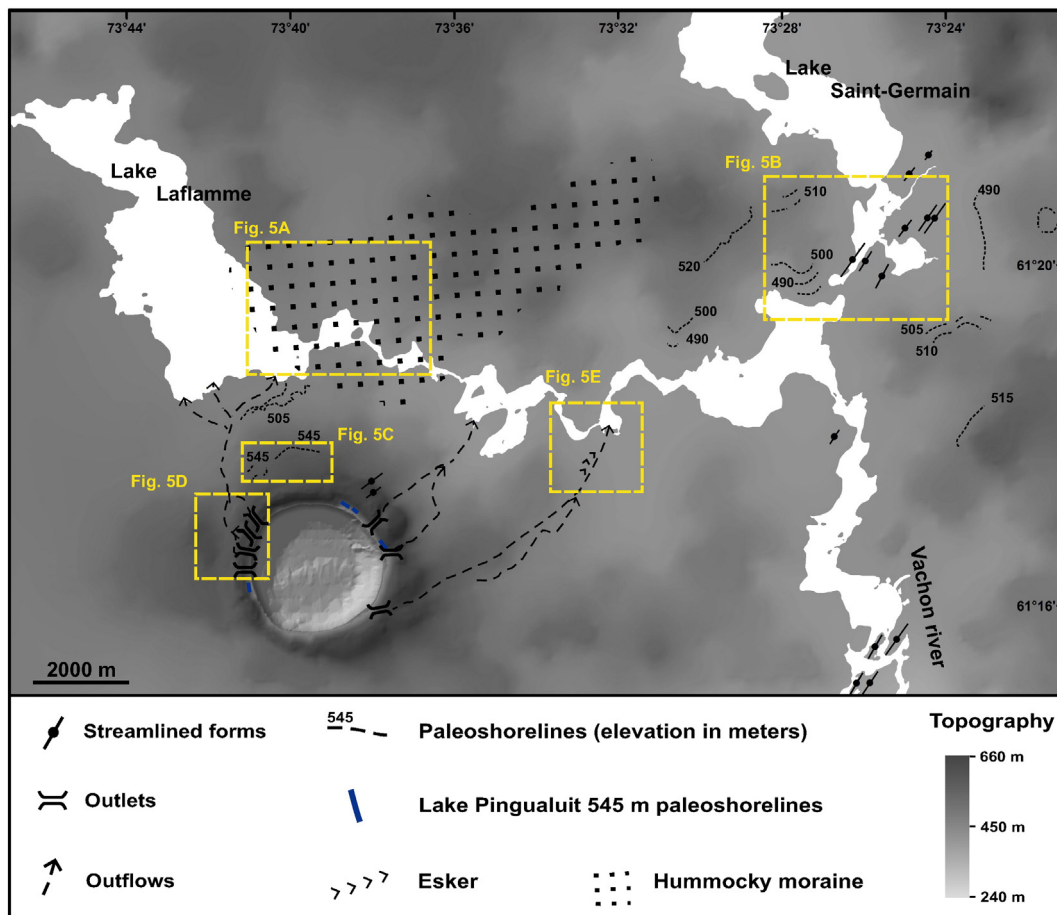


Fig. 4. Geomorphological map of the Pingualuit Crater Lake basin illustrating the identified glacial, deglacial, and hydrological landforms (see text for details).

seismic data do not represent the entire sedimentary sequence because of the weak penetration of the signal in very coarse deposits (Fig. 10A and B). Furthermore, the strict environmental regulations for this highly protected area of the Pingualuit National Park constrain the use of a higher energy seismic source (Guyard et al., 2011). The three seismic units have been observed only in the deep basin of the crater (Fig. 11A and B). The surface of slopes and the plateau is characterized by very low acoustic penetration with mid-amplitude reflection on top followed by a rapid deterioration of the signal. The very low penetration indicates the presence of many cobbles and/or boulders (Moussawi and Tessier, 1989) derived from rockfalls along the crater walls. Blocks and boulders present on the slopes of the crater also cover the submerged slopes and the plateau in the lake. The three units and two mass movement deposits described below are labeled from oldest to most recent (Fig. 10C). The generic mass movement terminology used indicates deposits or traces related to mass wasting according to their acoustic signature (e.g., Schnellmann et al., 2005, and references therein; Guyard et al., 2007). The interpretation of the seismic units follows the deep basin core description and discussion of Guyard et al. (2011, 2014).

5.1. Units 1 and 2 – glaciolacustrine deposits

Unit 1 is the lowest unit in the Lake Pingualuit sedimentary sequence. It is characterized by low acoustic penetration and the absence of reflections. Irregular high-amplitude small reflections are locally identifiable thereby contributing to the chaotic aspect of this unit. The base of unit 1 is not defined because of the weak penetration of the signal. This unit is observed only in the deepest part of the deep basin and

is located mainly where other units are visible. The maximal depth of the top of this unit attained ~5.75 m below the lake floor (Fig. 10C).

Unit 2 is characterized by high amplitude parallel reflections with poorly defined lateral limits. This unit is also observed only in the deeper part of the deep basin (Fig. 11A). The thickness of unit 2 varies from <1 to 4 m. In the sector where the 2007 core was recovered, the thickness of this unit reaches ~1 m and is present from ~3 m below the lake floor (Fig. 10).

Based on previous interpretation of similar acoustic facies and detailed sedimentology analyses, units 1 and 2 suggest a glaciolacustrine sedimentation phase associated with a decrease in discharge linked with the retreat of the LIS (Eyles and Mullins, 1997; Van Rensbergen et al., 1999; Guyard et al., 2011, 2014). At the coring site, these units correspond to finely laminated silts with dropstones interstratified with several massive sand layer intervals from 270 to 710 cm (Guyard et al., 2014). This facies and its glacial sediments are interpreted as high meltwater and sediment discharge with a lower influence of LIS detritic inputs at the top corresponding to unit 2. Units 1 and 2 probably correspond to the last stages of the retreat of the LIS margin, during which a semipermanent ice cover on the lake was still supplied by residual ice from the disintegrating and retreating glacier (Black et al., 2010; Guyard et al., 2011, 2014).

5.2. Unit 3 and mass movement deposits

Unit 3 is characterized by a low amplitude reflection and appears as a thick semitransparent and chaotic acoustic facies. Sediments of unit 3 cover about 25% of the basin and reach a maximum thickness of 3–4 m

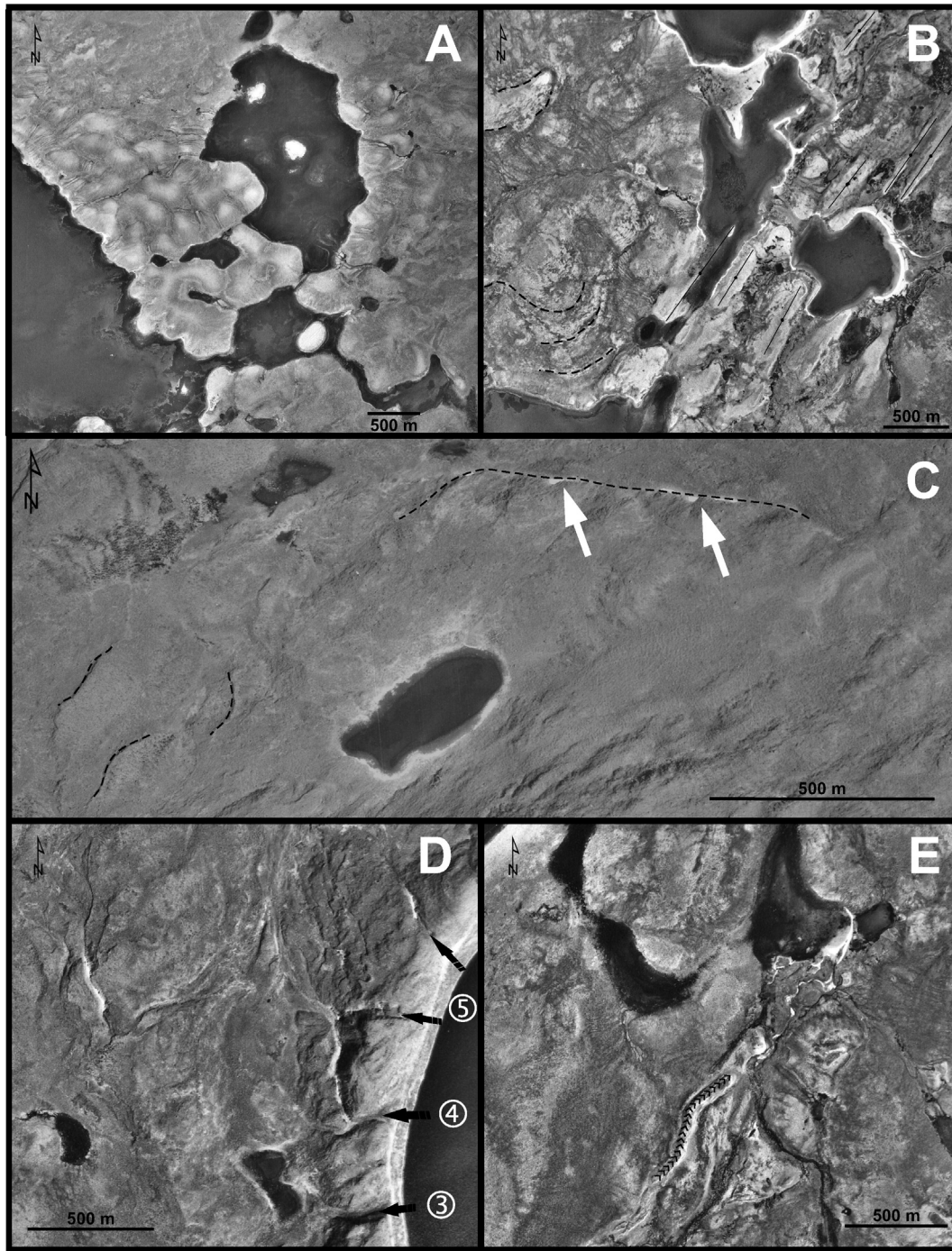


Fig. 5. Aerial photographs of glacial/deglacial and hydrological landforms in the Pingualuit Crater Lake basin. (A) Hummocky moraines in the sector of Lake Laflamme; (B) streamlined forms (black lines) and paleoshorelines (dashed lines) in the southern part of Lake St-Germain; (C) paleoshorelines (~545 m; dashed lines) on the external slopes of the Pingualuit Crater and snow banks persisting during summer (white arrow); (D) northwest outlets (black arrow) of the Pingualuit Crater Lake and associated outflow channels; (E) esker (multiple black chevrons) and terminal part of outflow channel linked to outlet 10.

in its deepest part (Fig. 11B). At the coring site, the thickness of this unit is about 2.5 m.

Mass movement deposits 1 (MM1) constitute the most chaotic and scarcely describable acoustic facies. These mass movement deposits are characterized by high amplitude chaotic and discontinuous reflections (overlapping hyperbolae) laterally disrupted by low amplitude and semitransparent lenses. A few meters below the top, these deposits are no longer observable owing to the chaotic configuration of the sediments, potentially coupled with the presence of coarse sediments and/or boulders, causing a weakening of the acoustic signal (Fig. 10).

According to this description, these deposits have acoustic characteristics typical of debris flows (Prior et al., 1984), but the limited correlation between acoustic profiles and the weak penetration of the signal limits this interpretation. Mass movement deposits 1 are present mainly in the northern and eastern parts of the crater at the base of the slopes and in the deep basin. Owing to the characteristics of this deposit, it is impossible to observe other units under MM1 with the seismic source used in this study. However, the contact between MM1 and underlying units 1 and 2 indicate that they were disturbed and probably eroded by this mass movement (Fig. 10C).

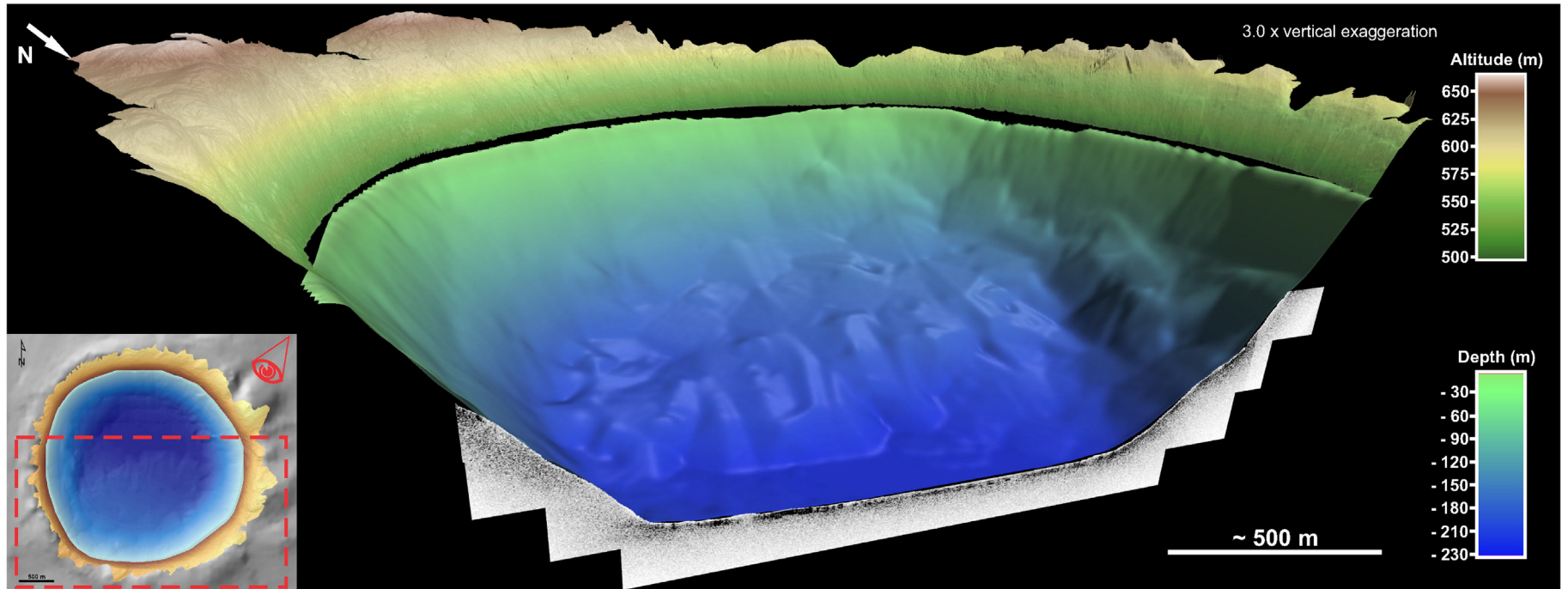


Fig. 6. A coupled topography–bathymetry model of the southern part of the Pingualuit Crater (dashed red frame) with an east–west seismic-reflection profile illustrated in Fig. 3. Mid-resolution bathymetry obtained by interpolation between seismic transects and high-resolution topography generated from LiDAR data. (For interpretation of the references to color in this figure legend, the reader is referred to the web version of this article.)

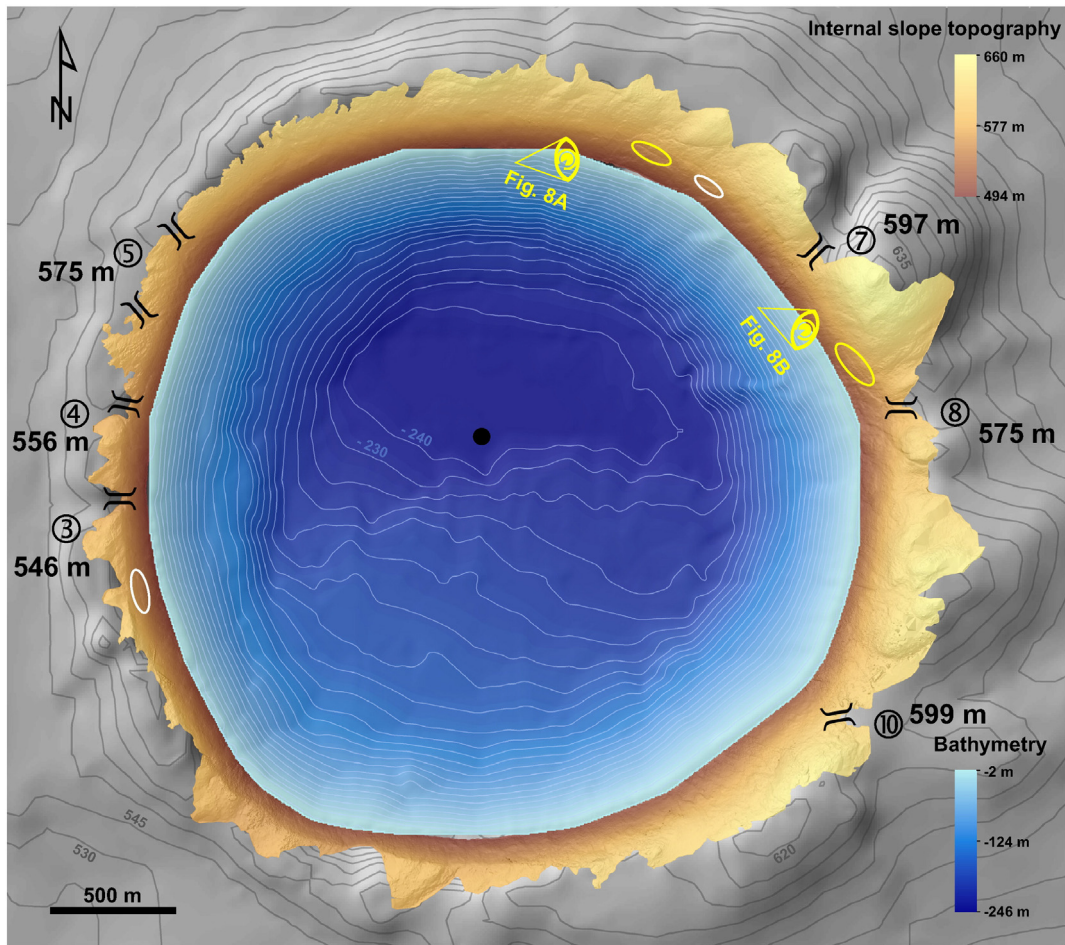


Fig. 7. DEM of the Pingualuit Crater using high-resolution topography of the internal slopes and mid-resolution bathymetry. Elevation of the crater rim channels are indicated in meters (asl) (black brackets) and paleoshorelines at 545 m asl are highlighted with white and yellow ellipses. The paleoshorelines highlighted with yellow ellipses are also illustrated in Fig. 8A and B. The yellow eyes represent the field of view illustrated in Fig. 8A and B. The black dot indicates the position of the coring site in the deep basin of the lake. (For interpretation of the references to color in this figure legend, the reader is referred to the web version of this article.)

Mass movement 2 deposits (MM2) consist of a chaotic to transparent seismic facies (Fig. 10C). The surface of MM2 is fairly smooth with occasional small hummocks where profiles cross the mass movement deposit. Its surface is also more irregular than the top of the underlying layer. Furthermore, MM2 does not overlay the other units but relies only on the surface of slopes and the plateau. Mass movement deposits 2 are observed in three types of bathymetric configurations (Fig. 11C): (i) at the base of steep slopes at the level of the plateau and in the deep basin mainly in the eastern part of the crater; (ii) on the shallower slopes between the plateau and the deep basin, in the south-central part of the crater; (iii) on the steep slopes in the western sector of the crater. In this area, MM2 reaches a maximum thickness of ~20 m, but elsewhere it ranges between 1 and 15 m in thickness. Mass movement deposits 2 were not observed in contact with the other identified units (Fig. 10).

The description of MM1 and MM2 indicates two distinct mass movement events in the Pingualuit Crater Lake. The first one, at the root of MM1 deposits, preceded MM2 and occurred after the deposition of seismic units 1 and 2, as indicated by the remobilization of these units by this first event. Unit 3 is probably the most recent deposit in the lake, though it could be concomitant with MM2. Indeed, unit 3 coincides with a mass movement deposit composed of folded and reworked glacial material and characterized by an erosive contact at its base (Guyard et al., 2011). Furthermore, both units have seismic characteristics with important similarities: low amplitude and transparent seismic facies. Finally, MM2 and unit 3 could be linked to a single depositional

event that occurred about 4200 cal BP (Guyard et al., 2014). Guyard et al. (2014) recently suggested a rotational slide based on the microsedimentological observation such as contorted sandy layers and internal deformations.

6. Discussion

6.1. Deglaciation in the Pingualuit Crater Lake area

Aerial photography focused on the Pingualuit Crater Lake basin reveals glacial streamlined forms and hummocky moraines, which respectively reflect the orientation and deglacial conditions of the last glaciation in the study area. The overall northeastern direction of all the observed streamlined forms attests to a main glacial Payne flow (azimuth 45°) following the Ungava flow (azimuth 110°) in the crater area during the last glaciation (Bouchard, 1989b; Daigneault and Bouchard, 2004). Glacial lineaments with close orientations (NNE–SSW) were also mapped by Clark et al. (2000) in this sector north of Ungava.

Hummocky moraines are generally deposited at the margins of the LIS and have been mainly observed in the Great Plains of North America (Gravenor and Kupsch, 1959; Parizek, 1969; Clark et al., 1996; Mollard, 2000; Boone and Eyles, 2001; Evans et al., 2014). In the Ungava Peninsula, the majority of hummocky moraines are located and gathered in the western part of the peninsula around the presumed position of the ice divide line. According to Daigneault (2008), these moraines would correspond to the locations of the last remnants of

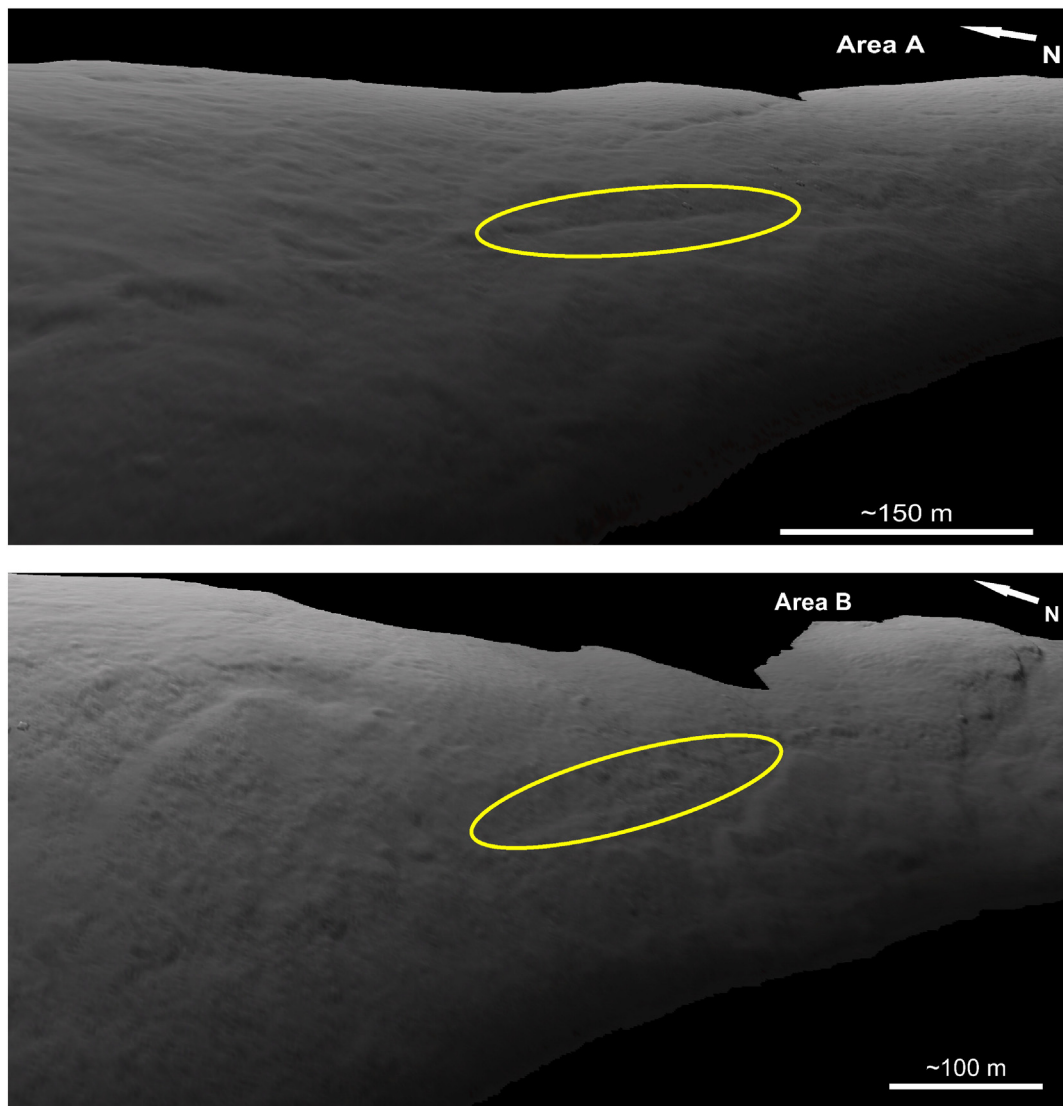


Fig. 8. Paleoshorelines at 545 m asl (yellow circles). The location of the two sites is illustrated in Fig. 7. (For interpretation of the references to color in this figure legend, the reader is referred to the web version of this article.)

ice. Furthermore, hummocky moraines are evidence of supraglacial or subglacial depositional processes tied to the stagnation of ice during ice sheet retreat (Gravenor and Kupsch, 1959; Stalker, 1960; Parizek, 1969; Johnson et al., 1995; Boone and Eyles, 2001; Daigneault, 2008). In the Pingualuit Crater area, hummocky moraines are relatively isolated, faintly extended and located farther away from the presumed position of the ice divide line (Figs. 1 and 4; Daigneault, 1997). This organization of moraines suggests the development of a stagnation zone during a rapid overall deglaciation of the Ungava Peninsula caused by the presence of glacial meltwaters (e.g., Evans, 2003; Daigneault, 2008). This scenario favors a glacial retreat model with fragmentation of the ice sheet into residual local ice masses during the last stage of deglaciation in this sector of Ungava, as also suggested by Clark et al. (2000). However, given that hummocky terrain is limited to the northeast sector of the study area (Fig. 4), it is likely that the stagnation zone did not occur on and immediately around Pingualuit Crater.

The paleoshorelines observed in the southern sectors of Lake Saint-Germain and Lake Laflamme are the remnants of the presence of a proglacial lake in the study area during deglaciation. Paleoshorelines identified at different elevations between 490 and 520 m asl (Fig. 4) provide further evidence for several periods of relative stable water level during the development and the regressing of the proglacial lake.

At that time, the ice front prevented drainage of glacial meltwaters to the south via the Vachon River, allowing the development of proglacial lakes (Daigneault, 2008). In the Lake Saint-Germain area, the elevation of the highest paleoshoreline indicates a proglacial lake with a maximum level of 520 m. The elevation of the paleodelta generated by outflows from Pingualuit Crater Lake that spread in the southern part of the Lake Laflamme area indicates a proglacial lake with a maximum level of 515 m (Fig. 12; Bouchard and Saarnisto, 1989). Nevertheless, the paleoshorelines observed on the external slopes of Pingualuit Crater at 545 m asl (Fig. 4) – corroborated by the paleoshorelines at ~540 m asl identified by Daigneault (1997) 2 km north of Cournoyer Lake and located at a distance of ~25 km east-northeast of the paleoshorelines at 545 m asl – may indicate the presence of a higher elevation proglacial lake. According to the measured elevation, the proglacial lake in the northern part of the Pingualuit area could have reached 545 m asl, ~45 m above the current level of Lake Laflamme (Fig. 12).

6.2. Deglacial history of Pingualuit Crater

Identifications of outflow marks, characterization of outlets, and identification of the paleoshorelines on the internal slopes of the crater allowed the establishment of a new deglaciation model for the

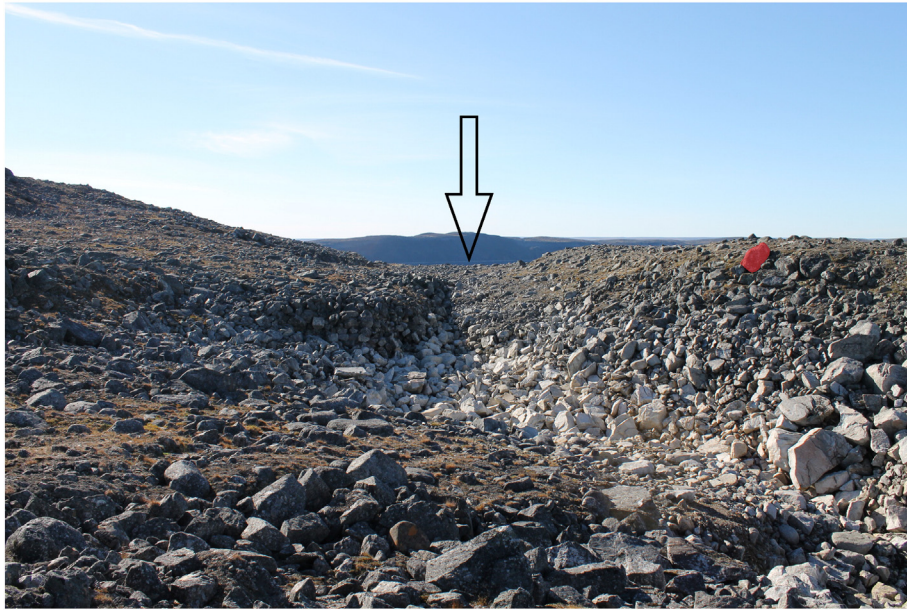


Fig. 9. Photograph presenting the mouth of outlet 10 with boulders washed and grouped by outflows. The black arrow indicates the Pingualuit Crater Lake in the background. The block underlined in red indicates the scale with a height of ~1.5 m. Photo credit: Alexandre Normandeau. (For interpretation of the references to color in this figure legend, the reader is referred to the web version of this article.)

Pingualuit Crater (Fig. 13). Two paleolake levels (574 and 514 ± 5 m) observed and described by Bouchard and Saarnisto (1989) are also used to support the model. However, the presence of paleoshorelines corresponding to these paleolake levels could not be confirmed by interpretation of LiDAR data. This model, presented in three main phases, is also based on the estimated NE direction of the noticeable esker (Fig. 5E) and the regional pattern of deglaciation as suggested by Daigneault (2008). The rapid glacial retreat occurred toward the SW with the main axis of the ice front oriented northwest to southeast (Bouchard and Saarnisto, 1989; Daigneault, 2008). The three phases discussed below do not correspond to periods of stagnation in the retreat of the ice front, but provide characteristic snapshots for each main phase of the Pingualuit Crater deglaciation.

During the first phase (phase I; Fig. 13) of deglaciation, glacial retreat affected the eastern sector of the crater, freeing a narrow band of the lake along the east coast. The eastern crater rim channels 7, 8, and 10 became ice-free and active as shown by outflow marks at their bases. Outlets 7 and 10 were probably fed for a reduced period of time on account of their high elevations at 597 and 599 m, respectively. Despite this short-lived activity, outlets 7 and 10 appear to have drained a significant amount of water into the proglacial Lake Laflamme and/or the Vachon River, as revealed by well-defined outflow channels at the base of each outlet. Furthermore, the esker observed in the downstream section of the channel system linked to outlet 10 indicates a subglacial drainage system independent of and prior to the drainage of the Pingualuit Crater Lake during the glacial retreat. The subglacial flows could result from outburst floods when the crater lake drained through outlet 10 below the ice sheet. As suggested by Guyard et al. (2011), the subglacial lake could have been supplied by meltwater inflows from the surrounding glacier under warm basal conditions and may thus have drained through highest outlets during an outburst floods. In this way, the flows generated by outburst flood of the subglacial crater lake could be an additional cause of well-defined channels linked to outlets 7 and 10 and the construction of the esker associated with channels located downstream of outlet 10. Outlet 8 received continuous overflow throughout phase I owing to its lower elevation (575 m). Lake levels were close but higher than the elevation of channel 10 (599 m) at the beginning of phase I and remained higher than the elevation of channel 8 (575 m) until its end, maintaining continuous drainage of the lake.

The LIS margin retreated toward the southwest until reaching the position shown in phase II, leading to the opening of crater rim channels 5 (Fig. 13). During phase II, equal-elevation outlets 8 and 5 (575 m) drained both simultaneously supercritical highly erosive flows, as revealed by distinctively marked outflow channels linked to outlets on the external slopes of the crater (Bouchard and Saarnisto, 1989). Outflows toward outlets 5 allowed, for the first time, drainage of the lake by the western part of the crater, resulting in the formation of the connection with proglacial Lake Laflamme. Furthermore, the less pronounced channels linked to outlet 8 could indicate a precocious abandonment of this channel and a concentration of the drainage toward outlets 5 in the northwest sector of the crater (Bouchard and Saarnisto, 1989). Finally, the end of phase II coincides with the end of drainage by these outlets and the stagnation of lake level, leading to the development of the highest and poorly developed paleoshoreline (574 ± 5 m) observed by Bouchard and Saarnisto (1989) in the northern part of the crater (Fig. 12).

During phase III, the glacial retreat maintained its progression toward the southwest thereby successively releasing channels 4 and 3 (Fig. 13). Low-elevation channels 4 and 3 (respectively 556 and 546 m asl) allowed the drainage of the lake waters from their elevation at the beginning of phase III to ~574 m. Runoff from these outlets was transported from the base of the external slopes to the northwest and flows into proglacial Lake Laflamme. Lowering of the lake level below the threshold of channel 4 caused desertion of this outlet, with the lower channel 3 becoming the last active crater outlet. Phase III finished with the disappearance of the last remnants of the LIS in the crater perimeter, implying the cessation of glacial inputs to the lake. Guyard et al. (2011) dated the change from proglacial to postglacial conditions in the Pingualuit Crater Lake basin at ~6850 cal BP.

Bouchard and Saarnisto (1989) suggested the maintenance of a temporary surface hydrological connection between the Pingualuit Crater Lake and Lake Laflamme at the transition between proglacial and postglacial conditions to explain the presence of the single fish population in the crater lake, Arctic Char (*Salvelinus alpinus*; Delisle and Roy, 1989). This connection requires a constant outflow through outlet 3 after phase III, requiring in turn the upkeep of lake waters at the level of the channel 3 threshold (Fig. 12; 546 m asl). Prolonged maintenance of the lake level around 546 m is confirmed by the paleoshoreline at

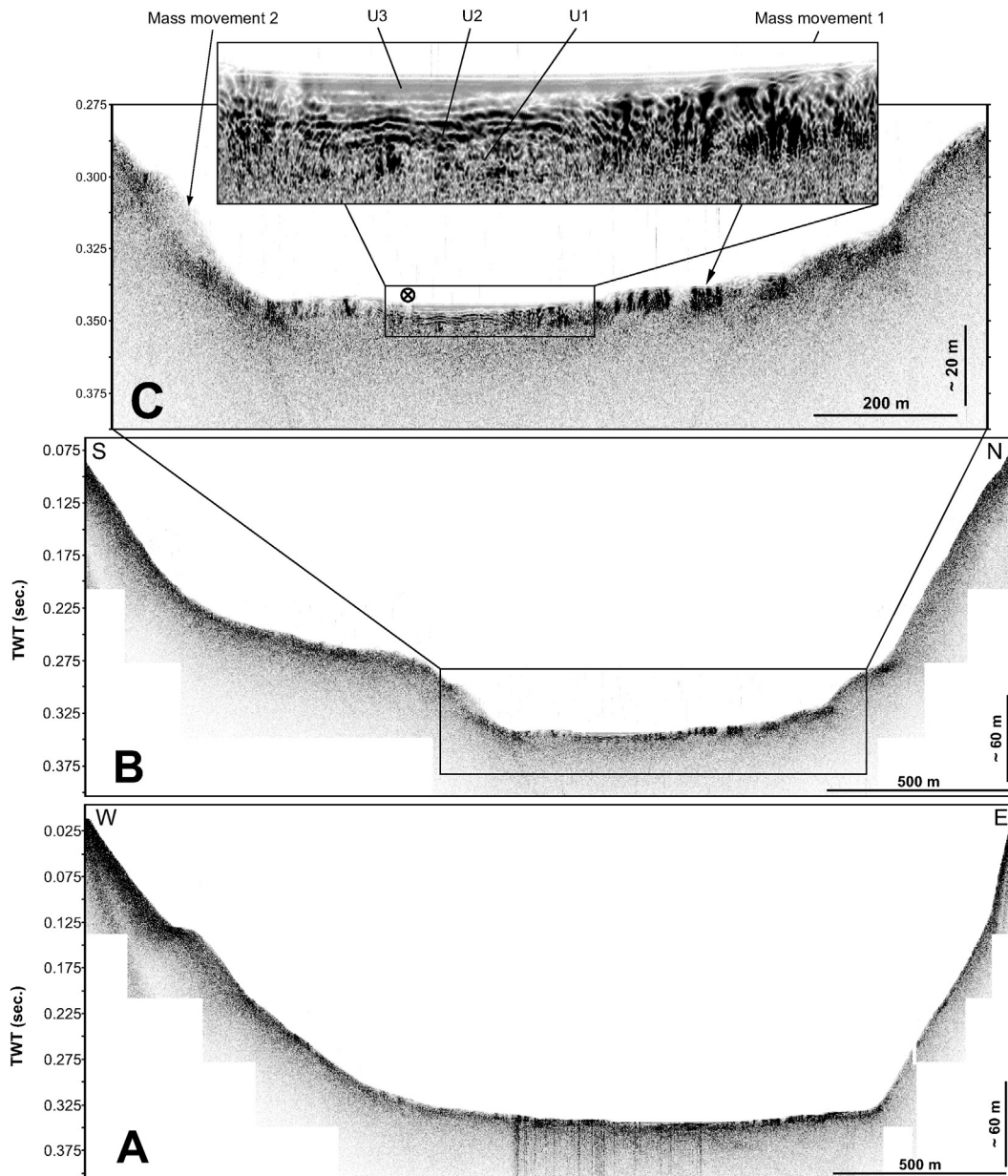


Fig. 10. Seismic lines (location in Fig. 3) from an east-west (A) and a north-south (B) profile illustrating in (A) and (B) typical profiles of the seismic reflection of the crater with the very low acoustic penetration; and in (C) the two mass movement deposits (mass movements 1 and 2) and the three seismic units (U1, U2, and U3) identified in the deep basin of the Pingualuit Crater. The cross indicates the coring site.

545 m asl distinctly observed with LiDAR data south of channel 3 and in the northern part of the crater (Fig. 8). The postglacial hydrological connection between the two lakes and the fish migration into the crater could have been facilitated by proglacial Lake Laflamme reaching 545 m asl as mentioned above (Fig. 12). Finally, the postglacial exorheic phase of Pingualuit Crater Lake ends when the lake level descends below the threshold of channel 3, potentially giving way to a cryptorheic drainage phase and the current hydrologic configuration (Bouchard and Saarnisto, 1989).

Since the end of the exorheic phase, the lake waters continually declined to reach their current level (494 m asl), as revealed by the absence of distinct intermediate paleoshorelines. The poorly developed paleoshoreline observed by Bouchard and Saarnisto (1989) around 514 m constitutes nonetheless an exception to this progressive lowering (Fig. 12). The decline of the lake level within the cryptorheic regime could be explained by the intensification of groundwater flows caused by climate change in the eastern Canadian Arctic and/or the drainage

of the neighboring proglacial lake. Indeed, the glacial retreat in the southern part of the study area opens up the release of the Vachon River, which had been obstructed and thus was responsible for the development of the proglacial lake north of the crater. The release directs the drainage of the proglacial lake to the Ungava Bay through the Vachon River and causes the lowering of lakes Laflamme and St-Germain to present levels (~500 m asl) (Daigneault, 2008). As the Pingualuit Crater Lake and Lake Laflamme were linked by a north-south oriented fault plane allowing cryptorheic drainage between both lakes (Currie, 1965), the lowering of proglacial Lake Laflamme would have modified the hydrostatic equilibrium (Ouellet et al., 1989). This destabilization has led to increased outflow through the fault plane from the crater lake to Lake Laflamme, consequently lowering the Pingualuit Crater lake level. The modern shoreline of the lake forms a 10-m-wide bench of washed boulders (Bouchard and Saarnisto, 1989). This well-defined configuration seems to indicate a current period of lake level stability. Regardless of the exact mechanism

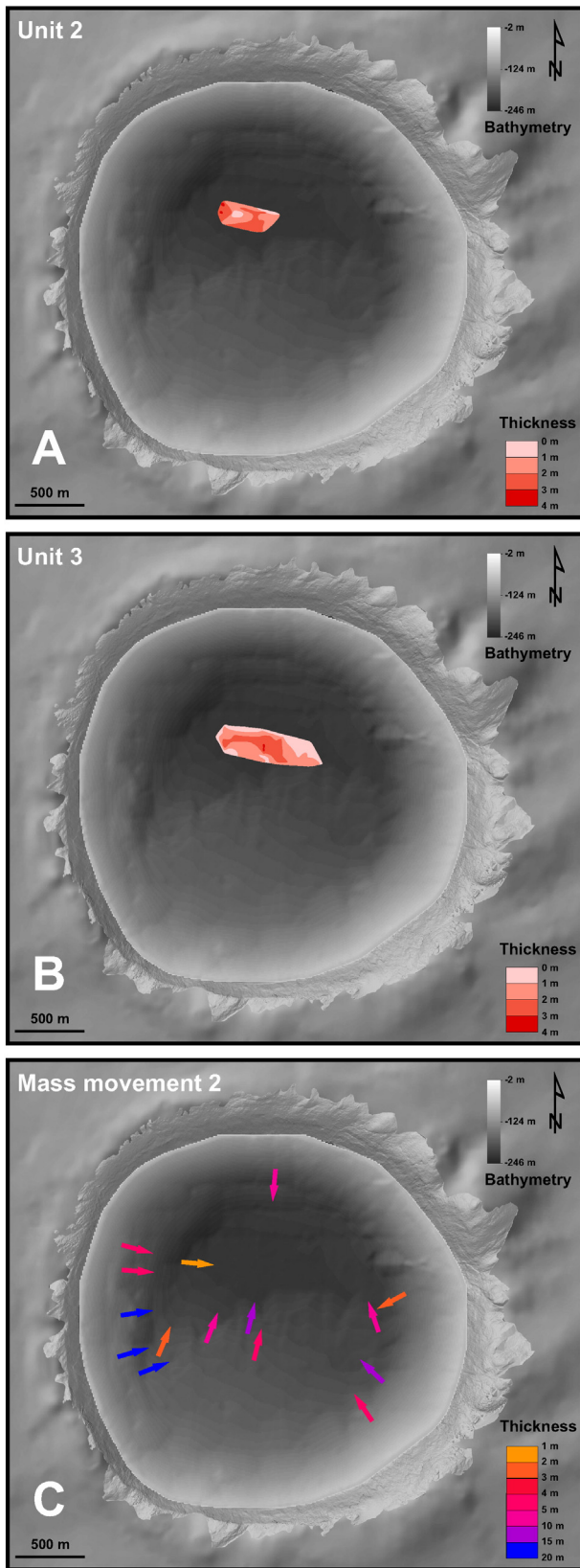


Fig. 11. Isopach maps from the Pingualuit Crater Lake. Maps (A) and (B) illustrate the thickness of units 2 and 3 in the deep basin, respectively. Map (C) is showing the estimated orientation and maximum thickness of multiple mass movement deposits linked to mass movement 2.

of lake lowering, the lake level dropped by 51 m since the end of the exorheic phase.

6.3. Deglacial and postglacial stratigraphy of the Pingualuit Crater Lake

Seismic units 1 and 2 (Fig. 10C) were probably deposited during phase III before the onset of postglacial conditions. Indeed, the glacialic sediments of these units clearly show a depositional environment with a semipermanent ice-covered lake still impacted by glacially derived detritic inputs from the last remnant ice blocks originating from the disintegration of the LIS (Fig. 13). The diminished glacial influence at the top of these units reflects the impending postglacial conditions (Guyard et al., 2014).

The two mass movement events that led to the deposition of MM1, MM2, and unit 3 (Fig. 10C) were probably triggered during or following the deglacial phase of the crater. According to the description of stratigraphy of unit 3 from Guyard et al. (2011), these deposits are composed of folded and reworked glacialic material probably accumulated on the slopes during the movement (advance/retreat) of the ice sheet. The chronology of these events indicates that deposition of MM1, preceding the depositional event linked to MM2 and unit 3 and dated around 4200 cal BP by Guyard et al. (2011), occurred after the deposition of sedimentary units 1 and 2 during phase III. The two mass movement events could have been triggered by a similar mechanism. The steep basin walls (26–35°) contribute greatly to the instability of the slopes, causing sediment redistribution through sliding and slumping (Dearing, 1997). Indeed, several models and studies, notably in small lakes, use and/or show instability or very low accumulation on the slopes beyond about 15% (~9°) (e.g., Hakanson, 1977; Hilton, 1985; Bennett, 1986). In the context of deglaciation, the retreat and disappearance of the thick ice sheet above the subglacial lake caused the reduction of water pressure in the lake and increased the exposure to weathering of the crater inner surface. These conditions, coupled with a rapid drop of lake levels and the activation of outlets through the crater rim, could have favored instabilities of aerial and subaqueous slopes (Guyard et al., 2011). The combination of these mechanisms and the increase of glaciolacustrine deposits associated with deglaciation of the lake likely explain the presence of MM1 limited to the northern and eastern part of the crater. Earthquakes are also a possible trigger mechanism for mass movements in lakes (e.g., Schnellmann et al., 2002; Monecke et al., 2004; Guyard et al., 2007; Normandeau et al., 2013). Observation of multiple MM2 deposits at the level or at the foot of slopes at many sites (Fig. 11C) could indicate a simultaneous triggering generated by an earthquake. Indeed, the area is seismically active and an $M_s = 6.3$ earthquake was recorded around 120 km SW of the crater (60.12° N.; 73.60° W.) in 1989 (Adams et al., 1991). Furthermore, the seismic activity could have been increased by glacioisostatic rebound following the deglaciation in Ungava (Guyard et al., 2011). Inferring from the still very steep submerged slopes and the apparently low filling of the crater since its formation 1.4 Ma ago (potential accumulation of 93 m, according to Moussawi and Tessier, 1989, corresponding to an average and approximate sedimentation rate of 6.5 cm ka^{-1}), the occurrence of mass movement deposition appears to have been relatively low and associated with exceptional events (e.g., earthquakes). This low occurrence is mainly caused by the very low supply of material to the slopes of the lake, except during phases of glacial advance and retreat. Compared to Laguna Potrok Aike (southern Patagonia), which has similar characteristics to the Pingualuit Crater Lake (e.g., morphology and high latitude location), the units, defined by laterally continuous reflections, in the first 20 m of the sedimentary sequence of the deep lake basin are also associated with episodes of mass movements and higher sedimentation rates (Anselmetti et al., 2009) than the Pingualuit Crater Lake. According to these authors, six mass-flow events have taken place during the last ~9000 years. Furthermore, Kliem et al. (2013) and Lisé-Pronovost et al. (2014) showed the presence of mass movement deposits covering half of a 100-m composite sediment sequence from

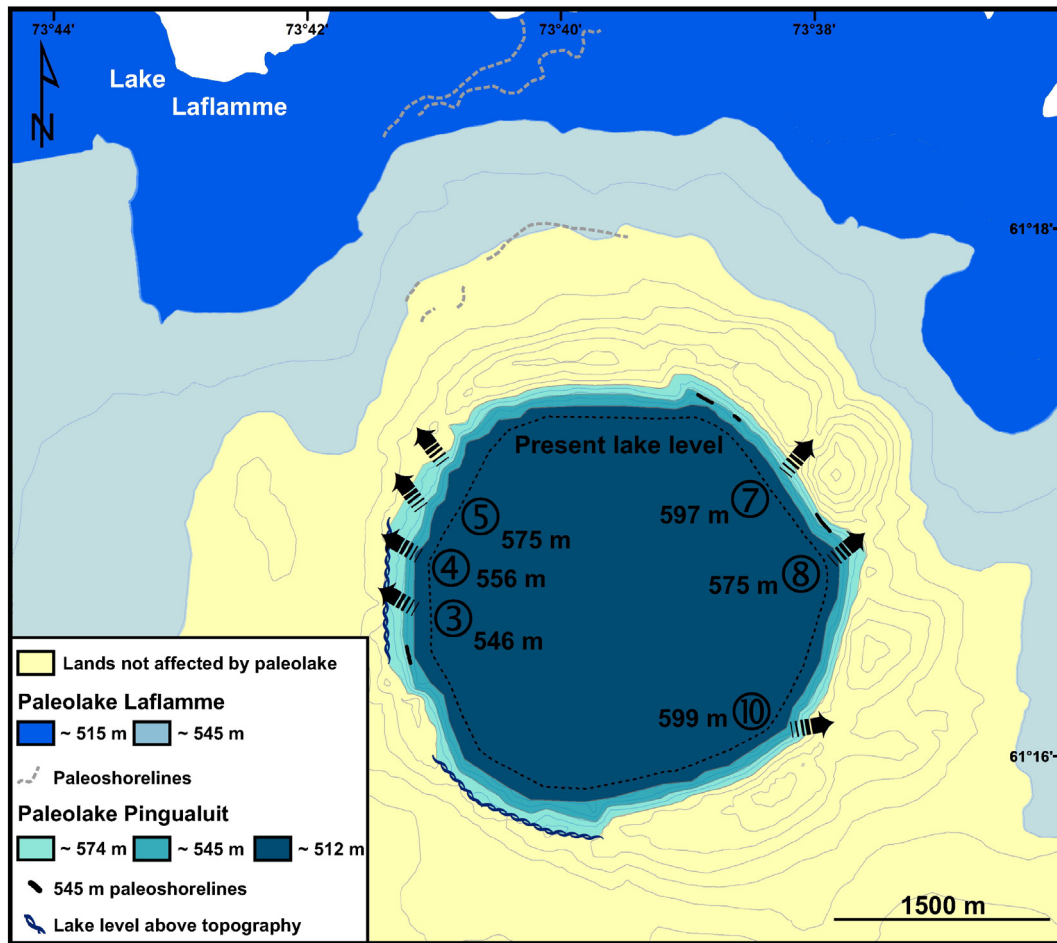


Fig. 12. Topographic map of the Pingualuit Crater Lake basin presenting the potential paleohydrology since the beginning of the deglaciation of the crater. The black arrows show the valleys involved in the lake drainage. The hypothetical proglacial lake at ~ 545 m is not illustrated in the southern part of the crater because of the lack of paleoshorelines observed near 545 m in this area.

the Laguna Potrok Aike Lake representing the last 51,200 cal BP. The different occurrence of mass movement events between both lakes is primarily explained by the periodic influx of sediments to the slopes of Laguna Potrok Aike Lake from a ~ 200 -km² watershed connected to this crater lake (Anselmetti et al., 2009) compared to a quasi-absent watershed for the Pingualuit Crater Lake.

Similarly, in Lake El'gygytgyn (Siberia) more than 400 mass movement deposits constitute $\sim 33\%$ of the Quaternary–Pliocene composite sediment record and the sedimentation rates discussed for this lake reveal values commonly higher compared to the Pingualuit Crater Lake, with sedimentation rates as high as 50 cm ka^{-1} (Nowaczyk et al., 2013; Sauerbrey et al., 2013). As suggested for Laguna Potrok Aike Lake, the difference in sedimentary dynamics between Lake El'gygytgyn and the Pingualuit Crater Lake is mainly caused by the much larger ~ 183 -km² watershed of Lake El'gygytgyn. In addition, well-stratified acoustic units were identified in the deepest part of Lake El'gygytgyn over the first 135 m of the seismic sequence and correspond to the sediment record covering the entire Quaternary (2.8 My; Niessen et al., 2007; Melles et al., 2012). On the other hand, the interpretation of the seismostratigraphy of the Pingualuit Crater Lake did not allow the identification of acoustically stratified units corresponding to postglacial lacustrine deposits on the slopes and at the base of the crater. This lack of well-stratified units and the weak signal penetration constitutes a major difference between the seismic data from the Pingualuit Crater Lake and the previously mentioned high-latitude lakes also studied for their paleoclimatic archives.

7. Conclusions

Seismic reflection data of Pingualuit Crater Lake allowed the identification of two units interpreted as glaciolacustrine units deposited during the final stages of deglaciation, as well as two postglacial mass movement deposits. Only a thin unit of high-amplitude parallel reflections is observed on the seismic data of Lake Pingualuit, indicating a low temporal resolution of sediment archives because of the low hemipelagic sedimentation rates. Indeed, all the deposits identified in this study derive from sedimentation during deglaciation and sediment reworking linked to postglacial sublacustrine mass movement events. In the Pingualuit Crater Lake, contrary to Lake El'gygytgyn and the Laguna Potrok Aike that are fed by small streams and periodic inflow, the absence of tributaries has greatly limited the accumulation of a high-resolution paleoenvironmental record since the retreat of the Laurentide Ice Sheet. Furthermore, a large number of cobbles and/or boulders are present on the submerged slopes and in the sedimentary deposits observed. The lack of seismic information beneath these units could indicate the presence of boulders below the glaciolacustrine units that prevents deeper signal penetration. The presence of these blocks could be explained by slope movements, which may have resulted from the balancing of slopes following impact cratering and/or by subglacial sedimentation during the last deglaciation in a complexly evolving subglacial lake.

The high-resolution topography of the internal slopes of the crater generated from LiDAR data permitted the identification of four

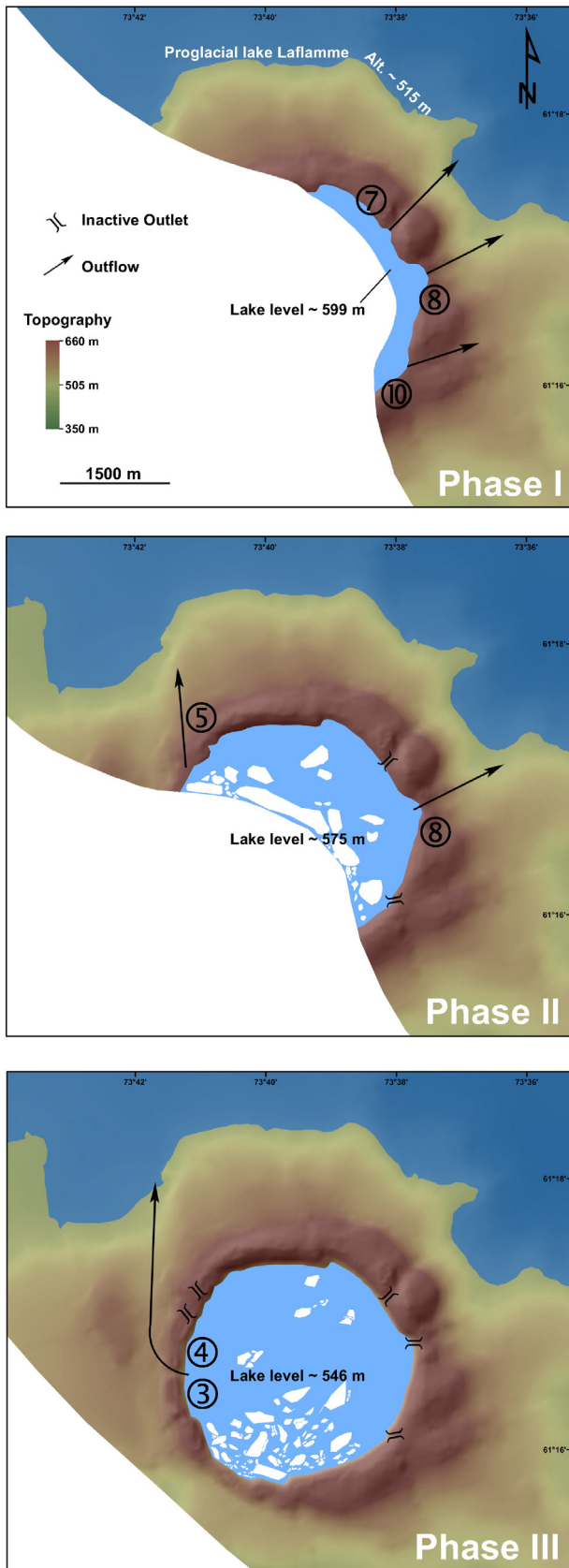


Fig. 13. Conceptual model for the deglaciation of the Pingualuit Crater Lake. The lake level indicated is the lowest lake level to maintain the exoreic drainage during each phase.

paleoshorelines with the same elevation of 545 m, confirming the presence of a paleolake level at 545 m. The elevation of various channels cutting the rim of the crater and serving as outlets for the drainage of lake waters have also been precisely identified on the LiDAR data. These observations coupled with the interpretation of aerial photographs provided the necessary information to present a new deglaciation model for the Pingualuit Crater and surroundings areas. The model proposes three main phases of lake drainage as channels opened following the retreat of the LIS front toward the southwest. The progressive activation of the seven outlets during the deglaciation led to a decrease of lake levels from elevations higher than 599 m (elevation of the highest outlet) to 545 m (elevation beneath the lowest outlet). The lowering of the lake to its present level (about 494 m asl) can be explained by an intensification of groundwater flow in a cryptorheic connection between the Pingualuit Crater Lake and the neighboring Lake Laflamme. This intensification possibly caused the modification of hydrostatic equilibrium between the two lakes following the drainage of the proglacial lake north of the crater.

Acknowledgments

The authors would like to sincerely thank Mireille Boulianne and Isabelle Raymond from Nunavik Parks and Markusi Qisiiq and Pierre Philie from the Parc National des Pingualuit for their help during planning stages, as well as Elijah Qisiiq, Mathew Argnak, Peter Qisiiq, Noah Annahatak, Elaisa Alaku, Bruno Tuniq, and Jobie Koneak for their help and dedication during the 2012 expedition. We thank Geneviève Philibert and Bryan Sinkunas (Université Laval) for their assistance during the seismic survey, as well as Catherine Cloutier and Dominique Turmel (Université Laval) and Stéfanie Van-Wierst (UQAR) for their help with LiDAR data processing. We are also thankful to Jacques Labrie and Elissa Barris (ISMER) for data processing and correcting the English of an earlier draft of the manuscript (respectively). Financial support for this research was provided by the Canadian Foundation for Climate and Atmospheric Sciences (CFCAS), the Natural Sciences and Engineering Research Council of Canada (NSERC), X-Strata Mine, the Canadian Foundation for Innovation (CFI), the Ministère de l'éducation, du loisir et du sport of Québec, the ArcticNet Network Centre of Excellence, and the Geological Society of America (GSA). The use of The Kingdom Suite® software was made possible by IHS. We are grateful to Editor R.A. Marston and three anonymous reviewers whose comments and suggestions improved the quality of this paper significantly. Finally, we dedicate this work to the memory of Isabelle Raymond.

References

Adams, J., Wetmiller, R.J., Hasegawa, H.S., Drysdale, J., 1991. The first surface faulting from a historical intraplate earthquake in North America. *Nature* 352, 617–619.

Anselmetti, F.S., Ariztegui, D., De Batist, M., Catalina Gebhardt, A., Haberzettl, T., Niessen, F., Ohlendorf, C., Zolitschka, B., 2009. Environmental history of southern Patagonia unravelled by the seismic stratigraphy of Laguna Potrok Aike. *Sedimentology* 56, 873–892.

Bennett, K.D., 1986. Coherent slumping of early postglacial lake sediments at Hall Lake, Ontario, Canada. *Boreas* 15, 209–215.

Black, J.L., Hausmann, S., Pienitz, R., St-Onge, G., Guyard, H., Salonen, V.-P., Lavoie, M., Girard-Cloutier, A.-M., Luoto, T., 2010. Reconstruction of Paleoenvironmental Changes from Pingualuit Crater Lake Sediments during Glacial–Interglacial Cycles MIS 1 to MIS 8: A Long-Term Terrestrial Record from the Canadian Arctic. *European Geophysical Union, Vienna, Austria*.

Black, J.L., Edlund, M.B., Hausmann, S., Pienitz, R., 2012. Small freshwater thalassiosiroid diatoms from Pleistocene sediments of Pingualuit Crater Lake, northern Québec (Canada), including description of *Cyclotella pingualuitii* sp. nov. *Diatom Res.* 27, 53–63.

Boone, S.J., Eyles, N., 2001. Geotechnical model for great plains hummocky moraine formed by till deformation below stagnant ice. *Geomorphology* 38, 109–124.

Bouchard, M.A., 1989a. Stratigraphie et sédimentation sous- et pro-glaciaire au lac du cratère du Nouveau-Québec. In: Bouchard, M.A. (Ed.), *L'histoire naturelle du Cratère du Nouveau-Québec* Collection Environnement et Géologie vol. 7. Université de Montréal, pp. 225–235.

Bouchard, M.A., 1989b. Englaciation et glaciation du cratère du Nouveau-Québec, un modèle théorique. In: Bouchard, M.A. (Ed.), *L'histoire naturelle du Cratère du*

- Nouveau-Québec Collection Environnement et Géologie vol. 7. Université de Montréal, pp. 139–163.
- Bouchard, M.A., Marcotte, C., 1986. Regional glacial dispersal patterns in Ungava, Nouveau-Québec. *Geological Survey of Canada, Paper* 86-1Bpp. 295–304.
- Bouchard, M.A., Marsan, B., 1989. Description générale du cratère du Nouveau-Québec. In: Bouchard, M.A. (Ed.), *L'histoire naturelle du Cratère du Nouveau-Québec* Collection Environnement et Géologie vol. 7. Université de Montréal, pp. 37–58.
- Bouchard, M.A., Saarnisto, M., 1989. Déglaciation et paléo-drainages du cratère du Nouveau-Québec. In: Bouchard, M.A. (Ed.), *L'histoire naturelle du Cratère du Nouveau-Québec* Collection Environnement et Géologie vol. 7. Université de Montréal, pp. 165–189.
- Bouchard, M.A., Marsan, B., Péloquin, S., Fortin, G., Saarnisto, M., Shilts, W.W., David, P.P., Fliszár, A., 1989. Géologie glaciaire du cratère du Nouveau-Québec. In: Bouchard, M.A. (Ed.), *L'histoire naturelle du Cratère du Nouveau-Québec* Collection Environnement et Géologie vol. 7. Université de Montréal, pp. 101–138.
- Brigham-Grette, J., Melles, M., Minyuk, P., 2007. Overview and significance of a 250 ka paleoclimate record from El'gygytgyn Crater Lake, NE Russia. *J. Paleolimnol.* 37, 1–16.
- Bruneau, D., Gray, J.T., 1997. Écoulements glaciaires et déglaciation hâtive (ca 11 ka BP) du nord-est de la péninsule d'Ungava, Québec, Canada. *Can. J. Earth Sci.* 34, 1089–1100.
- Clark, C.D., Knight, J.K., Gray, J.T., 2000. Geomorphological reconstruction of the Labrador Sector of the Laurentide Ice Sheet. *Quat. Sci. Rev.* 19, 1343–1366.
- Clark, P.U., Licciardi, J.M., MacAyeal, D.R., Jenson, J.W., 1996. Numerical reconstruction of a soft-bedded Laurentide Ice Sheet during the last glacial maximum. *Geology* 24, 679–682.
- Clark, P.U., Dyke, A.S., Shakun, J.D., Carlson, A.E., Clark, J., Wohlfarth, B., Mitrovica, J.X., Hostetler, S.W., McCabe, A.M., 2009. The last glacial maximum. *Science* 325, 710–714.
- Currie, K.L., 1965. The geology of the New Quebec crater. *Can. J. Earth Sci.* 2, 141–160.
- Daigneault, R.-A., 1993. Quaternary geology. *Geology of the eastern Cape Smith Belt: Parts of the Kangiqsujuaq, cratère du Nouveau-Québec, and lacs Nuvilik map areas, Québec. Commission Géologique du Canada, Mémoire* 438, pp. 96–99.
- Daigneault, R.-A., 1997. Géologie des formations en surface, région du cap de Nouvelle-France, du cratère du Nouveau-Québec et de Kangiqsujuaq, Québec-Territoires du Nord-Ouest. *Commission géologique du Canada, carte* 1863A.
- Daigneault, R.-A., 2008. Géologie du Quaternaire du nord de la péninsule d'Ungava, Québec. *Commission géologique du Canada, bulletin* 533p. 115.
- Daigneault, R.-A., Bouchard, M.A., 2004. Les écoulements et le transport glaciaires dans la partie septentrionale du Nunavik (Québec). *Can. J. Earth Sci.* 41, 919–938.
- Dearing, J.A., 1997. Sedimentary indicators of lake-level changes in the humid temperate zone: a critical review. *J. Paleolimnol.* 18, 1–14.
- Delisle, C.E., Roy, L., 1989. L'Ombre chevalier (*Salvinus alpinus*) du lac du cratère du nouveau Québec. In: Bouchard, M.A. (Ed.), *L'histoire naturelle du Cratère du Nouveau-Québec* Collection Environnement et Géologie vol. 7. Université de Montréal, pp. 261–276.
- Dyke, A.S., Prest, V.K., 1987. Late Wisconsinan and Holocene history of the Laurentide ice sheet. *Géog. Phys. Quatern.* 41, 237–263.
- Evans, D.J.A. (Ed.), 2003. *Glacial Land Systems*. Arnold Publisher, London (532 pp.).
- Evans, D.J.A., Young, N.J.P., Ó Cofaigh, C., 2014. Glacial geomorphology of terrestrial-terminating fast flow lobes/ice stream margins in the southwest Laurentide Ice Sheet. *Geol.* 204, 86–113.
- Eyles, N., Mullins, H.T., 1997. Seismic-stratigraphy of Shuswap Lake, British Columbia, Canada. *Sediment. Geol.* 109, 283–303.
- Girard-Cloutier, A.-M., 2011. Reconstitution paléobotanique et paléoclimatique en Ungava: analyse pollinique des sédiments du Cratère des Pingualuit (M.Sc thesis), Université Laval, Département de Géographie (68 pp.).
- Gravenor, C.P., Kupsch, W.O., 1959. Ice-disintegration features in western Canada. *J. Geol.* 67, 48–64.
- Gray, J.T., 2001. Patterns of ice flow and deglaciation chronology for southern coastal margins of Hudson Strait and Ungava Bay. In: MacLean, B.S. (Ed.), *Marine Geology of Hudson Strait and Ungava Bay, Eastern Arctic Canada: Late Quaternary Sediments, Depositional Environments, and Late Glaciale–deglacial History Derived from Marine and Terrestrial Studies*. Geological Survey of Canada Bulletin, pp. 31–55.
- Gray, J.T., Lauriol, B., 1985. Dynamics of the Late Wisconsin Ice Sheet in the Ungava Peninsula interpreted from geomorphological evidence. *Arct. Alp. Res.* 17, 289–310.
- Gray, J.T., Lauriol, B., Bruneau, D., Ricard, J., 1993. Postglacial emergence of Ungava Peninsula, and its relationship to glacial history. *Can. J. Earth Sci.* 30, 1676–1696.
- Grieve, R.A.F., Bottomley, G., Bouchard, M.A., Robertson, P.B., Orth, C.J., Attrep, M., 1991. Impact melt rocks from New Quebec crater, Quebec, Canada. *Meteoritics* 26, 31–39.
- Guyard, H., St-Onge, G., Chapron, E., Anselmetti, F., Francus, P., 2007. The AD 1881 Earthquake-triggered a slump and late Holocene flood-induced turbidites from proglacial lake Bramant, Western French Alps. In: Lykousis, V., Sakellariou, D., Locat, D. (Eds.), *Submarine Mass Movements and Their Consequences*. Kluwer-Springer, pp. 279–286.
- Guyard, H., St-Onge, G., Pienitz, R., Francus, P., Zolitschka, B., Clarke, G.K.C., Hausmann, S., Salonen, V.-P., Lajeunesse, P., Ledoux, G., 2011. New insights into Late Pleistocene glacial and postglacial history of northernmost Ungava (Canada) from Pingualuit Crater Lake sediments. *Quat. Sci. Rev.* 30, 3892–3907.
- Guyard, H., Francus, P., St-Onge, G., Pienitz, R., Hausmann, S., 2014. Microsedimentological investigation of subglacial and deglacial sediments from Pingualuit Crater Lake (Ungava, Canada). *Can. J. Earth Sci.* 51 (21), 1084–1096.
- Hakanson, L., 1977. The influence of wind, fetch and water depth on the distribution of sediments in Lake Vanern, Sweden. *Can. J. Earth Sci.* 14, 397–412.
- Hilton, J., 1985. A conceptual framework for predicting the occurrence of sediment focusing and sediment redistribution in small lakes. *Limnol. Oceanogr.* 30, 1131–1143.
- Johnson, M.D., Mickelson, D.M., Clayton, L., Attig, J.W., 1995. Composition and genesis of glacial hummocks, western Wisconsin, USA. *Boreas* 24, 97–116.
- Kliem, P., Enters, D., Hahn, A., Ohlendorf, C., Lisé-Pronovost, A., St-Onge, G., Wastegård, S., Zolitschka, B., the PASADO Science Team, 2013. Lithology, radiocarbon dating and sedimentological interpretation of the 51 ka BP lacustrine record from Laguna Potrok Aike, southern Patagonia. *Quat. Sci. Rev.* 71, 54–69.
- Lajeunesse, P., 2008. Early Holocene deglaciation of the eastern coast of Hudson Bay. *Geomorphology* 99, 341–352.
- Lauriol, B., Gray, J.T., 1987. The decay and disappearance of the late Wisconsin ice sheet in the Ungava Peninsula, northern Québec, Canada. *Arct. Alp. Res.* 19, 109–126.
- Ledoux, G., Lajeunesse, P., Philibert, G., Sinkunas, B., Guyard, H., St-Onge, G., Hausmann, S., Pienitz, R., 2011. Morpho-stratigraphy of Pingualuit Crater Lake, Ungava Peninsula, Nunavik. 41th Arctic Workshop. Montréal, Canada, p. 179.
- Lisé-Pronovost, A., St-Onge, G., Gogorza, C., Jouve, G., Francus, P., Zolitschka, B., the PASADO Science Team, 2014. Rock-magnetic signature of precipitation and extreme runoff events in south-eastern Patagonia since 51,200 cal BP from the sediments of Laguna Potrok Aike. *Quat. Sci. Rev.* 98, 110–125.
- Lisiecki, L.E., Raymo, M.E., 2005. A Pliocene–Pleistocene stack of 57 globally distributed benthic $\delta^{18}O$ records. *Paleoceanography* 20, PA 1003.
- Luoto, T.P., Salonen, V.-P., Larocque-Tobler, I., Pienitz, R., Hausmann, S., Guyard, H., St-Onge, G., 2013. Pro-and postglacial invertebrate communities of Pingualuit Crater Lake, Nunavik (Canada), and their paleoenvironmental implications. *Freshw. Sci.* 32, 951–963.
- Matthews, B., 1967. Late Quaternary land emergence in northern Ungava, Québec. *Arctic* 20, 176–202.
- Melles, M., Brigham-Grette, J., Minyuk, P.S., Nowaczyk, N.R., Wennrich, V., DeConto, R.M., Anderson, P.M., Andreev, A.A., Coletti, A., Cook, T.L., Haltia-Hovi, E., Kukkonen, M., Lozhkin, A.V., Rosén, P., Tarasov, P., Vogel, H., Wagner, B., 2012. 2.8 million years of Arctic climate change from Lake El'gygytgyn, NE Russia. *Science* 337, 315–320.
- Mollard, J.D., 2000. Ice-shaped ring-forms in Western Canada: their airphoto expressions and manifold polygenetic origins. *Quat. Int.* 68, 187–198.
- Monecke, K., Anselmetti, F.S., Becker, A., Sturm, M., Giardini, D., 2004. The record of historic earthquakes in lake sediments of Central Switzerland. *Tectonophysics* 394, 21–40.
- Moussawi, A., Tessier, G., 1989. L'épaisseur des sédiments au fond du Lac du Cratère du Nouveau-Québec: relevés géophysiques. In: Bouchard, M.A. (Ed.), *L'histoire naturelle du Cratère du Nouveau-Québec* Collection Environnement et Géologie vol. 7. Université de Montréal, pp. 199–222.
- Niessen, F., Gebhardt, C.A., Kopsch, C., Wagner, B., 2007. Seismic investigation of the El'gygytgyn impact crater lake (Central Chukotka, NE Siberia): preliminary results. *J. Paleolimnol.* 37, 49–63.
- Normandeau, A., Lajeunesse, P., Philibert, G., 2013. Late-Quaternary morphostratigraphy of Lake St-Joseph (southeastern Canadian Shield): evolution from a semi-enclosed glaci-marine basin to a postglacial lake. *Sediment. Geol.* 295, 38–52.
- Nowaczyk, N.R., Haltia, E.M., Ulbricht, D., Wennrich, V., Sauerbrey, M.A., Rosén, P., Vogel, H., Francke, A., Meyer-Jacob, C., Andreev, A.A., Lozhkin, A.A., 2013. Chronology of Lake El'gygytgyn sediments – a combined magnetostratigraphic, palaeoclimatic and orbital tuning study based on multi-parameter analyses. *Clim. Past* 9, 2413–2432.
- Occhietti, S., Parent, M., Lajeunesse, P., Robert, F., Govare, E., 2011. Late Pleistocene–early Holocene decay of the Laurentide Ice Sheet in Québec–Labrador. In: Ehlers, J., Gibbard, P.L., Hughes, P.D. (Eds.), *Developments in Quaternary Science*. Elsevier B.V., Amsterdam, The Netherlands, pp. 601–630.
- Optech Inc, 2008. ILLIRIS-3D Intelligent Laser Ranging and Imaging Systems [Online] Available from <http://www.optech.ca/id3techoverview-illiris.htm>.
- Ouellet, M., Pagé, P., Bouchard, M.A., 1989. Quelques aspects limnologiques du lac du cratère du Nouveau-Québec, Ungava. In: Bouchard, M.A. (Ed.), *L'histoire naturelle du Cratère du Nouveau-Québec* Collection Environnement et Géologie vol. 7. Université de Montréal, pp. 238–259.
- Parizek, R.R., 1969. Glacial ice-contact rings and ridges. *United States Contributions to Quaternary Research. Geological Society of America Special Papers* 123, pp. 49–102.
- Pienitz, R., Douglas, M.S.V., Smol, J.P., 2004. Long-term environmental change in Arctic and Antarctic lakes. In: Pienitz, R., Douglas, M.S.V., Smol, J.P. (Eds.), *Long-term Environmental Change in Arctic and Antarctic Lakes* Developments in Paleoenvironmental Research vol. 8. Springer, Dordrecht.
- Pienitz, R., Doran, P., Lamoureux, S., 2008. Origin and geomorphology of lakes in the polar regions. In: Vincent, W.F., Laybourn-Parry, J. (Eds.), *Polar Lakes and Rivers—Limnology of Arctic and Antarctic Aquatic Ecosystems*. Oxford University Press, Oxford, U.K., pp. 25–41.
- Prest, V.K., 1969. *Retreat of Wisconsin and recent ice in North America*. Department of Energy, Mines and Resources.
- Prest, V.K., 1975. Géologie du Quaternaire au Canada. *Chap. XII de Géologie et ressources minérales du Canada. Commission géologique du Canada, Série de la géologie économique* 1, pp. 752–852.
- Prior, D.B., Bornhold, B.D., Johns, M.W., 1984. Depositional characteristics of a submarine debris flow. *J. Geol.* 92, 707–727.
- Sauerbrey, M.A., Juschov, O., Gebhardt, A.C., Wennrich, V., Nowaczyk, N.R., Melles, M., 2013. Mass movement deposits in the 3.6 Ma sediment record of Lake El'gygytgyn, far east Russian Arctic. *Clim. Past* 9, 1949–1967.
- Saulnier-Talbot, E., Pienitz, R., 2010. Postglacial chironomid assemblage succession in northernmost Ungava Peninsula, Canada. *J. Quat. Sci.* 25, 203–213.
- Schnellmann, M., Anselmetti, F., Giardini, D., McKenzie, J., Ward, S.N., 2002. Prehistoric earthquake history revealed by lacustrine slump deposits. *Geology* 30, 1131–1134.
- Schnellmann, M., Anselmetti, F., Giardini, D., McKenzie, J., 2005. Mass movement induced fold- and thrust-belt structures in unconsolidated sediments in Lake Lucerne (Switzerland). *Sedimentology* 52, 271–289.
- Stalker, A.M., 1960. Ice-pressed drift forms and associated deposits in Alberta. *Geol. Surv. Can. Bull.* 57, 1–38.

- St-Onge, M.R., Lucas, S.B., 1990. *Geology, Cratère du nouveau-Québec, Québec. Geological Survey of Canada, Map 1731A.*
- Van Rensbergen, P., De Batist, M., Beck, C., Chapron, E., 1999. High-resolution seismic stratigraphy of glacial to interglacial fill of a deep glacial lake: Lake Le Bourget, North-western Alps, France. *Sediment. Geol.* 128, 99–129.
- Zolitschka, B., Anselmetti, F., Ariztegui, D., Corbella, H., Francus, P., Lücke, A., Maidana, N., Ohlendorf, C., Schäbitz, F., Wastegard, S., 2013. Environment and climate of the last 51,000 years – new insights from the Potrok Aike maar lake sediment archive drilling project (PASADO). *Quat. Sci. Rev.* 71, 1–12.